PUBLICATIONS OF THE WATER AND ENVIRONMENT RESEARCH INSTITUTE

3

Timo Huttula (ed.)

Systems analysis applications to water research — a Soviet-Finnish project

NATIONAL BOARD OF WATERS AND THE ENVIRONMENT, FINLAND
Helsinki 1989

PUBLICATIONS OF THE WATER AND ENVIRONMENT RESEARCH INSTITUTE

3

Timo Huttula (ed.)

Systems analysis applications to water research — a Soviet-Finnish project

NATIONAL BOARD OF WATERS AND THE ENVIRONMENT, FINLAND
Helsinki 1989

The author are responsible for the contents of the publication.
It may not be referred to as the official view or policy
of the National Board of Waters and Environment.

ISBN 951-47-3096-8
ISSN 0783-9472

Helsinki 1989 Valtion painatuskeskus

CONTENTS

492899K

PREFACE

This publication presents a part of results in water research obtained in the cooperation between USSR Academy of Sciences and Academy of Finland. The joint investigations have been carried out within the project 16. The project started 1983.

The project has four themes: 1) Development of optimum management rules for water resources systems, including lakes and reservoirs, 2) Development of models of snow cover and snowmelt runoff formation in the forest zone for operative management of water resource systems, 3) Development of monitoring systems for water bodies to receive information for control and optimum management of water quality, 4) Analysis of the ways to improve water quality using hydrodynamic models.

The results of this cooperation were discussed in the first Soviet-Finnish symposium on the system analysis application to water research in Moscow on 10—14 November 1986. The papers presented there are published in Mimeograph Series of NBWE, Finland, no. 27/1987.

The articles published now cover all the four themes. The articles have been chosen by both partners of the cooperation to represent the scientific results of the cooperation. The editor expresses his gratitude to all the contributors and office personnel who have made this publication possible. Special thanks to Mrs. Leena Pukkila for typing, Mrs. Tuulikki Sevon and Miss Päivi Vanhapelto for redrawing some of the figures and equations, and Mrs. Paula Ullakko for the layout.

Tampere, September 1989

Timo Huttula
The editor

THE DEVELOPMENT OF OPERATING RULES FOR THE VUOKSI RIVER BASIN

Dina Korobova[1], Valentin Poizner[1], Yuri Oziranskii[1], Yuri Plotkin[1], Andrew Egorov[1], Markku Maunula[2] and Reijo Porttikivi[3]

KOROBOVA D., POIZNER V., OZIRANSKII Y., PLOTKIN Y., EGORON A., MAUNULA M & PORTTIKIVI R. The development of operating rules for the Vuoksi river basin, Publication of the Water and Enviroment Research Institute, National Board of Waters and the Environment, Finland no. 3.

The work is aimed at the development of methodology for operation of multipurpose water resource systems in conditions of uncertainty, especially for flood and drought periods.

For the analysis of water resource systems operation the multireservoir regulation model developed in the USSR has been used. The inflow values of the major lakes of the Vuoksi River Basin were calculated from the outflow and water stage data for years 1941—1954 and 1956—1982.

The forecast calculations were made by using stepwise regression and as an example the inflow correlation coefficients of Lake Pielinen are presented in the paper. As a Case-study the possibilities for using the headwater lakes for flood control of Lake Saimaa have been investigated.

The results show that the multireservoir model can be used for studying the effect of different operational alternatives and for getting a good knowledge of the river system behaviour. The floods can be best controlled by requlating the Lake Saimaa but in severe flood situations the headwater lakes may be used for minimising the damages.

Index words: multireservoir regulation, water resources, multipurpose

[1] Water Problems Institute USSR Academy of Sciences, Sadovo-Chernogriazskaya ul., 13/3, 103064 Moscow, USSR

[2] The National Board of Waters and the Environment, PL 250, 00101 Helsinki, Finland

[3] The National Board of Waters and the Environment, The District Office of Kuopio, PL 49, 70101 Kuopio, Finland

1 INTRODUCTION

The main subject discussed in this paper is the development of guidelines for operating a water resource system in conditions of uncertainty, especially during flood and drought periods.

The Vuoksi River Basin is a transboundary river system for Finland and the USSR (Fig. 1). The development of the management policy of the River System, especially considering flood control, is a common goal for both countries. Joint affairs concerning the watercourse are dealt within the framework of the Finnish — Soviet Boundary Water Commission.

A major difficulty in the utilization of the Vuoksi River System is, on one hand, the

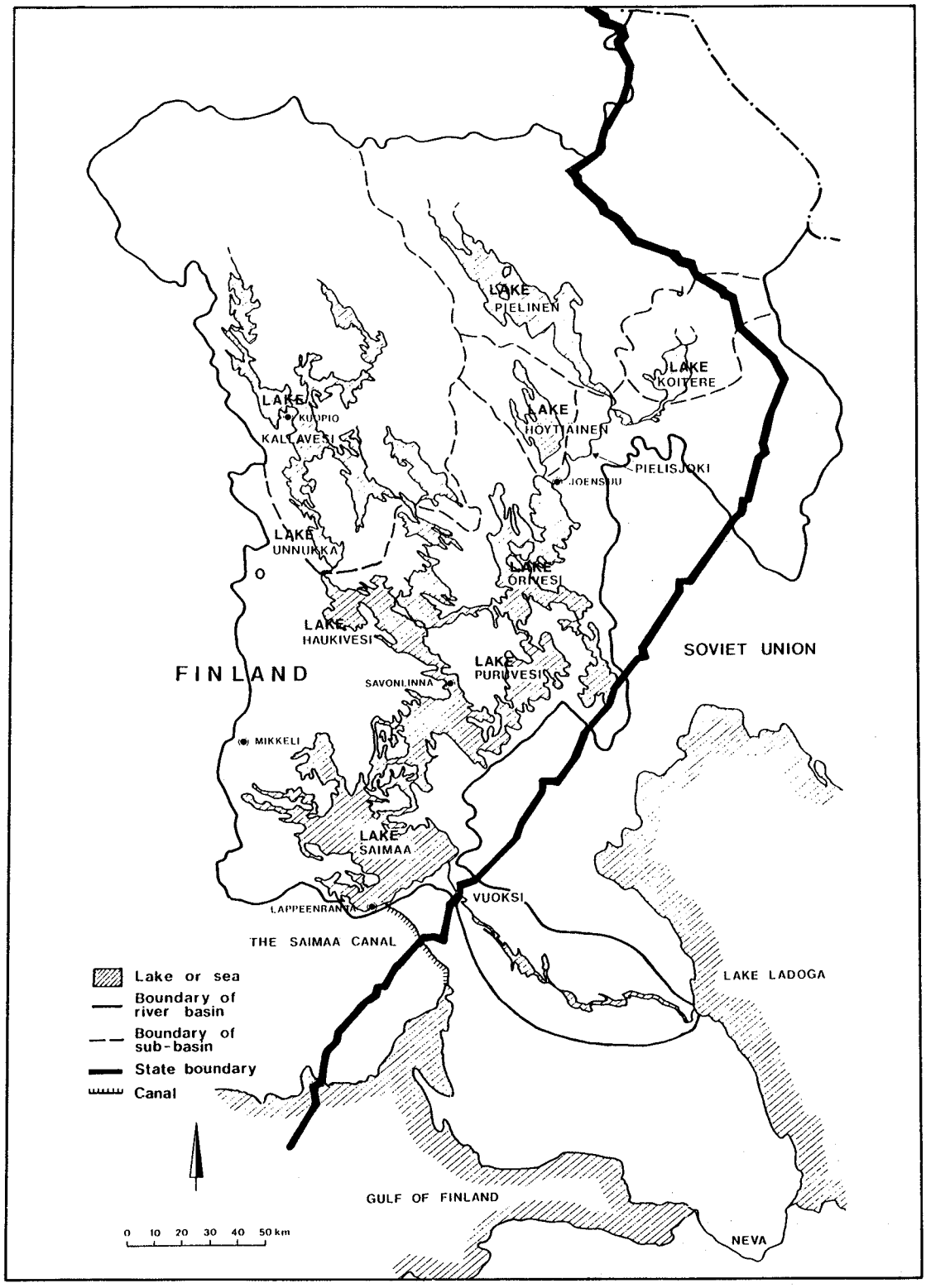

Fig. 1. The Vuoksi River Basin.

forecasting of exceptional flood and drought periods and, one the other hand, the compiling of operation rules in such a way that overall damages are minimized. During flooding, the main aim is to lower the highest water stages of Lake Saimaa and to avoid excessive discharges into the Vuoksi River.

2 THE HYDROLOGY OF THE VUOKSI RIVER BASIN

2.1 General description

The drainage area of the Vuoksi River Basin is 61 265 km^2 and the proportion of lake coverage is 19.8 %. The northern part of the River Basin comprises two large, adjacent tributaries, the Kallavesi (16 270 km^2) and Pielinen (20 975 km^2) lake chains, which discharge into the largest of the Finnish lakes, Lake Saimaa (see Fig. 1).

Other important tributaries are formed by Höytiäinen (1 425 km^2) and Koitere (6 795 km^2) basins. Waters leaving the Lake Saimaa flow through the River Vuoksi to Lake Ladoga, which is situated in the USSR. From Lake Ladoga waters are running through the River Neva to the Gulf of Finland. Saimaa is also connected to the Gulf of Finland by a navigation canal. The overall area of Lake Saimaa is 4 460 km^2, which can be subdivided into three main lake systems — Orivesi, Haukivesi and lower Saimaa, the water levels of which slightly differ from each other (Fig. 1).

The mean annual precipitation of the total catchment area is 590 mm and evaporation 405 mm. Normally the maximum water equivalent of snow is at the beginning of April. The average maximum is 150 mm and for the return period of 100 years the value is 240 mm.

Hydrological observations have been made in the Vuoksi River Basin over a rather long time period. For example the observations of the water levels have been made since the year 1847 in Lake Saimaa and the year 1863 in Lake Kallavesi.

The highest observed water level of Lake Saimaa in NN + 77.65 m in 1899 and the lowest water level is 74.28 m in 1942. The variation in water level of Lake Saimaa is unusually high among Finnish unregulated lakes, exceeding 3 m (Fig. 2). The mean discharge (MQ) of the Vuoksi River at the outlet of Lake Saimaa is 590 m^{3}s^{-1}, maximum (HQ) 1 190 m^{3}s^{-1} (in 1899) and minimum (NQ) 220 m^{3}s^{-1} (in 1942), (Table 1).

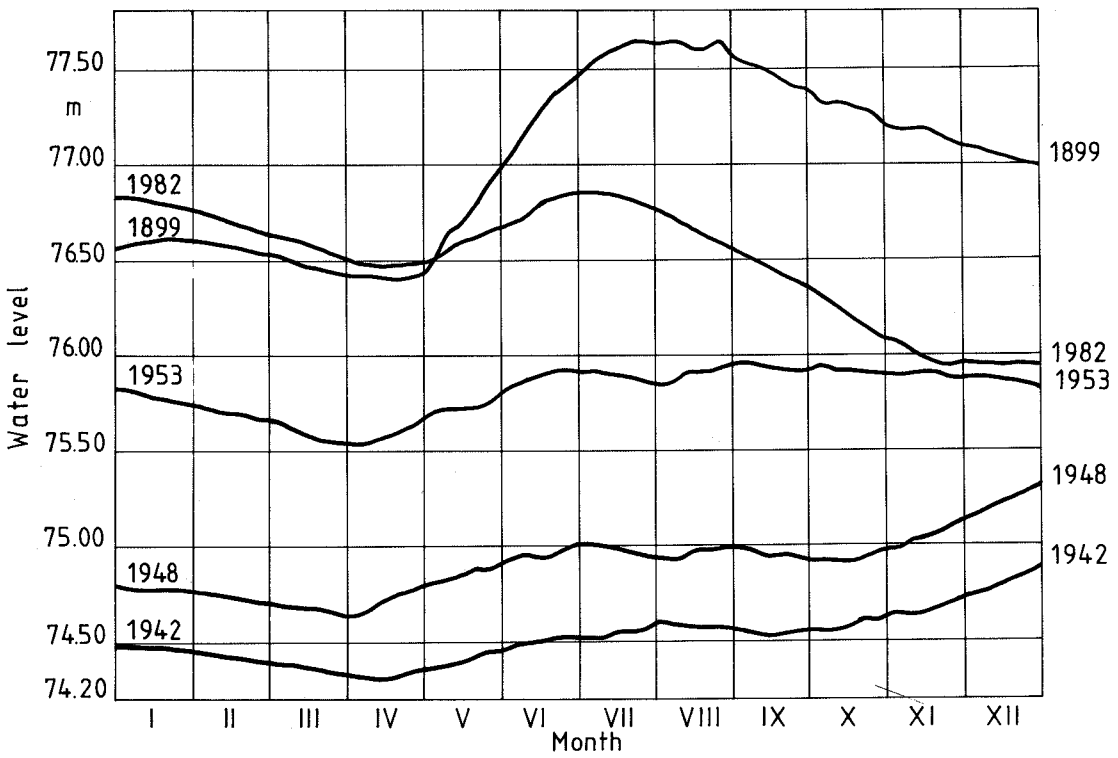

Fig. 2. Natural water level variations of Lake Saimaa.

Table 1. Hydrological data of the largest lakes in the Vuoksi River Basin and of Lake Ladoga.

Lake	Surface area at mean level	Mean depth	Volume between mean and minimum levels	Current water level annual variation cm		Discharge in 1961—80 m^3s^{-1}		
	km^2	m	10^6m^3	Mean	Maximum	MQ	HQ	NQ
Saimaa	4 368	14	3 672	68	161	554	1 115	165
Pielinen	960	9	665	119	168	231	545	45
Kallavesi	898	9	561	71	160	166	484	52
Unnukka	110	—	51	28	60	118	358	30
Höytiäinen	290	8	169	78	85	14	72	0
Koitere	181	6	173	154	215	73	263	1
Ladoga	17 840	51	15 000[1)]	74[1)]	164[1)]	2 540	10 687	45

[1)] Estimated on the basis of Lake Saimaa values

2.2 The management of the Vuoksi River System

Numerous flow regulations have been implemented in the Vuoksi River Basin. The largest regulated lakes of the Vuoksi River System are Kallavesi, Unnukka, Höytiäinen and Koitere. The lakes Saimaa and Pielinen are unregulated.

Water transportation has old traditions since the 1850's when the first Saimaa Canal was constructed to connect Lake Saimaa with the Gulf of Finland. Today the amount of transported goods through the Canal is about 1.6 million tons annually. The total amount timber floated yearly in the Vuoksi River System is about 2.5 million tons.

The hydropower plants of the Finnish part of the Vuoksi River Basin produce annually about 2 TWh or nearly 20 % of Finland's total hydropower production. The two greatest of those, Tainionkoski and Imatra power plants, produce about 1.3 TWh, which equals the total production of the Svetogorsk and Lesogorsk power plants in the Soviet part of the Vuoksi River System.

The Vuoksi River System is also important for fishing and recreation. In Lake Saimaa area there are about 41 000 recreational fishermen. The annual catch which includes professional fishing is about 5000 tons. The recreational use in the area has grown rapidly especially in the 1970's and 1980's. There are nowadays 100 000 summer dwellings on the 60 000 km long shoreline, the major part of which is privately owned. There are 3 000 km safely navigable channels which are well used for tourist cruises and boating. The total amount of boats is about 100 000 of which 20 000 are motor- and sailingboats.

More and more emphasis has been laid on the preservation of aquatic nature and scenic values of the lake area. There have been controversial opinions on impacts of lake regulation and water construction works on the Saimaa landlogged ringed seal (Phoca hispida Saimensis) and salmon (Salmo salar m. sebago) which both are relics in Lake Saimaa from its previous Baltic Sea phase.

Floods cause damages much more often than droughts due to the climatic conditions and the number of lakes in the Vuoksi River System. When water level is rising, the flooding first damages fields, forests and houses. In addition, Lake Saimaa is surrounded by numerous factories — mainly paper mills — which suffer remarkably from flood when it is at its worst. On the other hand, flood also causes remarkable damages on the Soviet side, when discharge in the River Vuoksi is great.

Therefore, the threat of damages on one hand and the impacts of prevention measures on the other hand in both countries have to be taken into consideration when planning and implementing flood protection.

The largest flow regulations in the Vuoksi River Basin are quite moderate. They all tend to lower the highest flood levels and raise the lowest water levels. When there is a threat of very great damages, a temporary permit for deviating from natural conditions can be applied from the Water Court. These temporary permits have been used in recent years for lakes Saimaa and Pielinen (Table 2).

By means of temporary permits it has been possible to reduce significantly flood damages. In consequence, these exceptional tappings have caused energy losses to hydropower plants both in

Table 2. The effect of temporary flood-regulations executed in the Vuoksi River Basin, Difference = Regulated − Natural.

	Maximum water level NN + m		Maximum discharge m^3s^{-1}	
	Natural	Difference	Natural	Difference
Lake Saimaa				
1962—3	76.79	−0.05	896	+213
1974—5	76.90	−0.12	932	+183
1981	76.85	−0.24	916	+7
1982	76.87	−0.36	922	−139
1984	76.62	−0.31	841	+67
Lake Pielinen				
1981	94.88	−0.29	546	+38
1982	94.52	−0.17	446	+2
1984	94.48	−0.42	435	+3

the USSR and Finland. The Finnish Government has compensated the energy losses to the Soviet Union.

A convention concerning the transboundary waters between the USSR and Finland was signed in 1964. According to this convention information concerning the anticipated discharges of the River Vuoksi are sent by the Finnish authorities weekly in advance to the Soviet hydropower station at Svetogorsk. The forecast for the following two months is sent monthly to the power station, as well.

2.3 The regulation of the Kallavesi Water System

The possibilities for regulation of Lake Kallavesi were first examined after the big flood occurring in the year 1924. The regulation plan has been revitalized by the agreement between Finland and the Soviet Union aiming at the reconstruction of the Saimaa Canal in the year 1962. The final impulse was given by Finnish government which in 1968 made a decision on the construction of deep water channel (sailing depth 4.2 m) from Varkaus to Kuopio, a distance of 75 km.

The main aim of the regulation plan for Kallavesi lake chain was to create a profitable technical solution for navigation from Saimaa to Kuopio. The plan was also aimed at promoting flood control, recreational use of lakes and water supply. The regulation was also to improve the energy production capacity of Varkaus power plant. The conditions for power plants in the Vuoksi River were not allowed to worsen on either side of the boundary line between the two nations.

Considering Lake Kallavesi the most essential fact was that the plan should be realized without causing damages along the thousands of kilometres long shoreline. Otherways the venture would have been suffocated in juridical process due to the numerous claims by the land owners.

The low water level during the navigation season was raised 0.2 m. This level can be guaranteed with 97 % certainty. In the 0.75 m zone between the mean high water level and the lowest navigation level the lake could be regulated freely. However, when water rises above the mean high level, extra releases must be conducted for ensuring that water level does not exceed the levels in respective condition in the natural state which should be verified by calculations.

It was not possible to raise Lake Unnukka to the level of Lake Kallavesi because in that case the protection of Varkaus paper and pulp industry from inundation would have become excessively costly. The solution was a 0.4 m raise of the Lake Unnukka from the prevailing mean water level. The raise was still remarkable considering the lessening of dredging costs for navigation. The water level raise caused to some extent damages for fields and forest land. Damages were paid for about thousand private estates.

3 MODEL DESCRIPTION

3.1 Initial information

The inflow values have veen calculated according to the water balance calculations from the outflow

and water stage data for the largest lakes of the Vuoksi River Basin: Kallavesi, Höytiäinen, Pielinen and Koitere. The calculations were made for periods 1941—1954 and 1956—1982. The monthly net inflows into Lake Saimaa from the surrounding smaller watersheds have been calculated so that the observed discharges of upstream lakes have been substracted from the total inflow of the Vuoksi River System. The inflows to Lake Unnukka have been calculated on the basis of the inflows to Lake Kallavesi.

Initial hydrologic series encompass periods of high- and lowflow (Fig. 3). Multiannual fluctuations are especially distinct in the Lake Saimaa where three eleven-year periods might be resolved — two lowflow periods 1941—1951 and 1963—1973 and one highflow period 1952—1962.

The inflow models were made by using stepwise regression equations (1)—(3), (Table 3). The equations were calculated according to the hydrological data for years 1953—1982. The inflow volume models for springtime were calculated for the period 1 April—31 July. The prediction dates are 1 February, 1 March and 1 April. The dependent

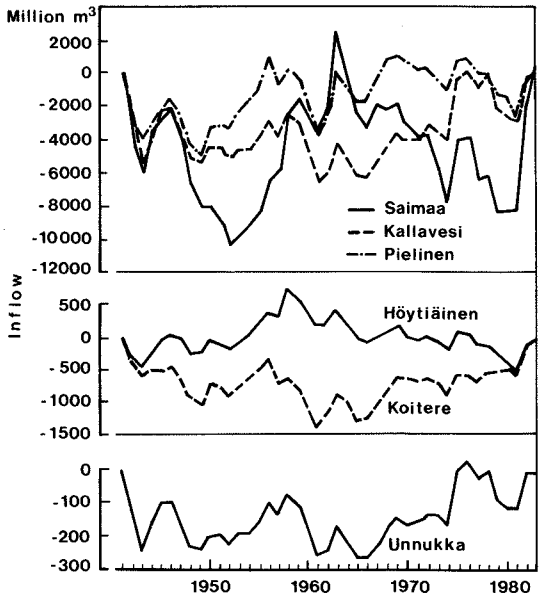

Fig. 3. Differential mass diagram curves of unregulated net inflow to the main lakes of the Vuoksi River Basin.

Table 3. The regression equations used to predict the inflow volume of Lake Saimaa.

Prediction date 1st of February:

$$V_{4-7} = -83.000 + 3.257\,Q_1 + 37.277\,(L_{1\,\text{Feb.}} + P_2 + P_3) + 30.564\,(P_4 - 34) + 45.108\,(P_5 - 40) + 12.133\,(P_6 - 62) + 6.678\,(P_7 - 67) \qquad R^2 = 88.36 \qquad (1)$$

Prediction date 1st of March:

$$V_{4-7} = -755{,}258 + 6.202\,Q_2 + 33.445\,(L_{1\,\text{Mar.}} + P_3) + 23.696\,(P_4 - 34) + 41.632\,(P_5 - 40) + 11.771\,(P_6 - 62) + 9.333\,(P_7 - 67) \qquad R^2 = 90.25 \qquad (2)$$

Prediction date 1st of April:

$$V_{4-7} = 2\,034.848 + 3.803\,(Q_3 - 415) + 34.550\,(L_{1\,\text{Mar.}} + P_3) + 33.204\,(P_4 - 34) + 43.525\,(P_5 - 40) + 11.804\,(P_6 - 62) + 5.810\,(P_7 - 67) \qquad R^2 = 82.81 \qquad (3)$$

where

V_{4-7} = total inflow volume from 1st of April to 31st of July, m^3s^{-1}

Q_1, Q_2, Q_3 = monthly mean inflow to Lake Saimaa in January, February and March, respectively, m^3s^{-1}

L_{1Feb}, L_{1Mar}, L_{1Apr} = water equivalent of the snow cover at the 1st of February etc., mm

P_1,...P_7 = Monthly precipitation from January to July, respectively, deviation from the monthly mean, mm

R^2 = correlation coefficient squared

variable is the volume of the inflow during the period 1 April—31 July. The independent variables are:

— the precipitations of April, May, June and July (mm) (decreased by the mean value)
— the mean inflow of the month preceding the prediction date (m^3s^{-1})
— the water equivalent of the snow cover in the prediction date increased by the anticipated precipitation during the period from the prediction date to 1 April (mm).

Three verification periods were used for testing the models, and they were the years 1923—1952, 1953—1982 and 1923—1982. The differences between the observed inflows and the predicted inflows for every year in the testing periods were calculated. When predicting the inflow values, the unknown precipitation parameters were substituted by the observed mean values.

3.2 Multireservoir regulation model

Presently, a great number of mathematical models — optimization and simulation, static and dynamic, stochastic and deterministic models — have been developed to explain the behaviour of water systems. Although all of them are viable, it is expedient to select a proper mathematical model type for a particular water resources system and a particular problem.

The type selected for this study is simulation model. This model allows us to obtain knowledge on water resources system behaviour under various conditions for further decision making (Velikanov et. al. 1983). In the model the "out-of-kilter" algorithm is used for optimal water flow distribution (Techn.Rep. 1970 and Bazaraa T. et. al. 1977).

The purpose of this model is to provide a water resources planner with the means for analyzing water storage and water allocation within a multireservoir or multibasin system. The model is also designed to provide flexibility in selection of operating rules for each reservoir.

The concept of this model is that the physical water system can be transformed into a network flow problem. The transformation is called a nodal system, where the real system's physical elements are presented as a combination of two possible network components, nodes and links. Typically, a link is a river reach, canal, or closed conduit with a specified direction of flow and a fixed minimum and maximum capacity. In order to make the network continuous certain additional nodes and links should be added to the system. These are initial storage and inflow nodes and links, end-of-time-interval desired storage links (operating rules), final storage nodes, balance of final storage and maximum reservoir capacity links, spill nodes and links and net balance nodes and links.

In addition, a priority ranking used to determine the allocation of water to meet the demands and to maintain water storage is assigned to each reservoir and demand.

The set of ranking priorities is assigned by the planner in dependence with the role and importance of a water demand or reservoir and with the hydrological state of the system. The hydrological state of the system may be defined in various ways, for example, on the basis of hydrological data on reservoirs and unregulated inflows for the beginning or for the end of the time interval, with the use of hydrological forecasts of without it, etc.

In the model the set of ranking priorities has been transformed into the transportation cost of a flow unit in the network. The "cost" of flow transportation between nodes does not contain economic significance, in this case it is the criterion which is in direct relationship with the reservoir or demand priority. Therefore, the relations between priorities are important, not the absolute values.

Some assumptions have been made in the model:

— unregulated inflows to the system: nodes are known for the time interval being simulated
— admissable reservoir storage fluctuations between the maximum and minimum capacities are specified by the model user
— spills occur only at nodes and are specified by the user
— the flow in all links varies between the maximum and minimum capacity specified by the user.

In accordance with the priorities assigned above the problem of determination of the minimum total cost of water transportation within the network may be written as follows.

$$\sum_{i}^{n}\sum_{j}^{n} C_{ij}Q_{ij} \tag{4}$$

where Q_{ij} is the flow from the node i to the node j, C_{ij} is the cost of transportation of the unit of flow from node i to node j and n is the number of nodes.

The following condition of mass balance conservation should be kept:

$$\sum_{i}^{n} Q_{ij} - \sum_{j}^{n} Q_{ji} = 0 \tag{5}$$

and the upper and lower limits on the outlet capacity of links should also be kept:

$$L_{ij} \leq Q_{ij} \leq U_{ij}, \tag{6}$$

where L_{ij} and U_{ij} are the lower and the upper boundaries of the outlet capacity of links.

Some modifications have been done in the model to adjust it to the problem of the analysis of the water resources system behaviour in the Vuoksi River Basin. These modifications have been necessitated mainly by the need to simulate the natural regime of lakes.

3.3 Formalisation of the Vuoksi River System by linear-nodal schemes

The use of the above described mathematical model to develop operating rules for the Vuoksi River Basin has demanded the development of linear-nodal schemes of the water system (Fig. 4) — a complete and a simplified one. The complete scheme incorporates six lakes (nodes 1—6), the outlet node (node 8), and the node locking the scheme with fictious demand in the node (node 7 -Lake Ladoga). The introduction of the demand with low priority allows one to control water surpluses in the lakes of the Vuoksi River Basin and to avoid extreme rise of their levels (Fig. 4).

The simplified scheme includes three main lakes of the system: Saimaa, Kallavesi and Pielinen, receiving about 90 % of the total inflow to the lake system (Table 4). The simplified scheme was found suitable for operational use. Unregulated inflow to Saimaa includes inflow from small watersheds.

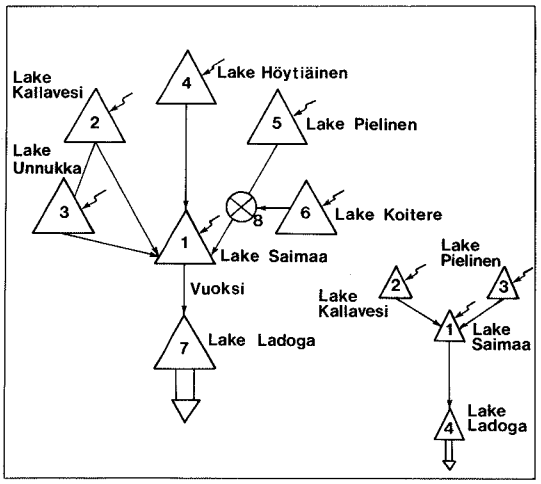

Fig. 4. The linear-nodal scheme of the Water System of the Vuoksi River Basin.

Table 4. Inflow distribution among lakes in the Vuoksi River Basin (1941—1954, 1956—1982).

Lake	Inflow %
Saimaa	35
Kallavesi	29
Pielinen	28
Koitere	4
Höytiäinen	3
Unnukka	1
Total	100

4 RESULTS

4.1 Adequacy of the Vuoksi River System Model

The verification computations show that the simulation model describes the behaviour of the Vuoksi River Basin with sufficient accuracy (Table 5). All differences between calculated and observed values of multiyear operational characteristics are within admissable limits.

Table 5. The results of verification computation for Lake Saimaa in 1941—1954 and 1956—1982. NM is natural mean level and DIFM is natural mean level — modelled mean level; SN, SM are standard deviations for natural and modelled levels, respectively.

Month	NM m	DIFM cm	SN cm	SM cm
I	75.55	−6	55	51
II	75.56	−2	53	51
III	75.54	+1	50	49
IV	75.48	+2	47	45
V	75.54	+2	45	44
VI	75.68	−2	48	46
VII	75.79	−1	49	48
VIII	75.78	−2	49	47
IX	75.73	+1	48	46
X	75.67	+3	52	46
XI	75.60	0	49	47
XII	75.61	−1	51	49

4.2 Flood forecast models

The use of inflow volume forecasts for a flood period may considerably improve the quality of management of lake system. In major lake systems,

where flood period is quite long, the inflow forecast have to be calculated for several shorter periods, in this case for months.

Existing procedures for estimation of runoff distribution during floods are based on assessment of the dates for one or two characteristics (e.g. the flood volume, the dates of the beginning and the end of the flood period, etc.). The difficulty in issuing such a forecast ensues from the fact that the seasonal runoff distribution depends greatly on weather conditions, which can not be determined with sufficient accuracy in advance. Therefore, without long-term prediction of weather conditions, deterministic means of runoff distribution prediction for a flood period will remain unreliable and practically unused.

To solve this problem it is possible to use probabilistic means to predict flood runoff distribution by means of conditional curves of distribution. The development of curves is illustrated by the following example of the unregulated inflow to lake Pielinen.

First of all, the pair correlation coefficients of monthly and total inflows are calculated to determine the closest relations (Table 6).

Based on Table 5 we can consider the following inflows as the arguments of conditional curves for various months: for April — total inflow (April—July), for May — inflow from May to July, for June and July — inflow from June to July. From Table 7 we can see that the probabilistic forecasts by using conditional curves are suitable for May, June, and July.

The use of conditional curves doesn't give substantially better results in April because the beginning date of flood period in spring varies so much from year to year.

Conditional curves of probability, developed for a particular month, represent a family of parallel straight lines, differing only by conditional mean values which depend on the argument values. It should be noted that the described method of the development of conditional curves can be applied only to conditional distributions with moderate asymmethry and absolute values significantly greater than zero.

4.3 Case: The use of upstream lakes in the flood control of Lake Saimaa

Time series simulated by the model represent the years 1941—1954 and 1956—1982. The year 1955 was not included because of the lack of discharge observations at Lake Koitere. For the simulation, monthly objectives of water level elevation were prepared also for Lake Pielinen and Lake Saimaa although those lakes are not regulated at present. The aim of the simulation was to study the effects of regulation measures in upstream lakes onto the joint behaviour of the lakes. Computational time step was one month.

Table 6. Matrix of the inflow correlation coefficients, Lake Pielinen.

Period	April	May	June	July	April—July	May—July	June—July
Apr	1						
May	0.11	1					
Jun	−0.04	0.49	1				
Jul	0.05	0.43	0.65	1			
Apr—Jul	0.37	0.82	0.76	0.75	1		
May—Jul	0.06	0.85	0.82	0.78	0.95	1	
Jun—Jul	0.00	0.50	0.91	0.90	0.83	0.89	1

Table 7. Parameters of unconditional and conditional distribution of inflows for the flood period, Lake Pielinen.

Month	Mean inflow	Mean square deviation		Conditional/ unconditional
		unconditional	conditional	
	km^3	km^3	km^3	
April	0.410	0.195	0.181	0.93
May	1.050	0.315	0.166	0.53
June	0.560	0.205	0.085	0.41
July	0.396	0.193	0.084	0.44

The calculations demonstrate that, e.g. for the winter flood of 1974—1975, it would have been possible to drop the flood stages of Lake Saimaa in the end of 1974 mainly by increasing discharges of the Vuoksi River, but a drop in the flood stages in the spring of 1975 would have been possible only by regulation of the upstream lakes. In that case the maximum discharge into the Vuoksi River would have been only 853 m^3s^{-1} during the whole flood period of 1974—1975 (Table 8).

In the simulation during the 11 month period from 1 Aug. 1974 to 30 June 1975 in average a flow of 27 m^3s^{-1} was stored in Lake Pielinen and 19 m^3s^{-1} in Lake Kallavesi. The benefit was a decrease in the flood stages of Lake Saimaa by 22 cm to the level of NN + 76.66 m expressed in monthly mean values. Lake Kallavesi rose to the level of NN + 82.85 m and Lake Pielinen to NN + 94.70 m. According to the preliminary damage estimation, Kallavesi rose about 30 cm too high and, correspondingly, more floodwater could have been stored in Lake Pielinen (Table 8).

Table 8. Maximum water level and discharge of Lakes Saimaa, Pielinen and Kallavesi and simulated results compared with natural and observed monthly mean values. diff = simulated — observed.

	Lake Saimaa			
	Maximum water level NN + m (m)		Maximum discharge (m^3s^{-1})	
Year	observed	diff.	observed	diff.
1943	76.29	−0.30	737	+101
1954	76.07	−0.18	671	+178
1962	76.76	−0.57	886	− 37
1963	76.72	−0.72	873	− 24
1974	76.73	−0.21	875	− 26
1975	76.88	−0.22	928	− 75
1981	76.82	−0.37	905	− 56
1982	76.83	−0.47	909	− 60

	Lake Pielinen			
Year	observed	diff.	observed	diff.
1943	94.69	−0.87	322	− 81
1954	94.26	−0.44	265	+ 14
1962	94.64	+0.20	403	−124
1963	94.06	+0.65	213	+ 14
1974	94.35	−0.25	300	− 21
1975	94.38	+0.32	282	− 43
1981	94.56	+0.01	341	− 62
1982	94.30	+0.62	284	− 5

	Lake Kallavesi			
Year	observed	diff.	observed	diff.
1943	82.48	−0.60	467	− 72
1954	82.10	−0.22	311	+118
1962	82.24	+0.36	360	− 15
1963	81.68	+0.12	184	+ 21
1974	82.12	−0.25	376	+113
1975	82.21	+0.64	365	− 65
1981	82.43	+0.04	420	− 71
1982	82.31	−0.37	374	− 74

5 THE ROLE OF THE MODEL IN DEVELOPING THE MANAGEMENT OF THE VUOKSI RIVER SYSTEM

An action plan for flood control of the Vuoksi River Basin is under preparation. The aim of the plan is to develop arrangements and procedures by which the benefit of both countries can be quaranteed. In the plan separate alternatives will be studied for reducing flood damages.

To estimate the operational possibilities of the model the boundary conditions for the regulation like the flood damages of different lakes at different water level elevations and the juridical considerations have to be taken into account.

In Figure 5 there is a diagram of flood damages in Lake Saimaa as a function of water level. The damages increase considerably when water rises over the level 76.50 m. On the other hand flood causes also remarkable damages on the Soviet side, when the discharge in the River Vuoksi is great.

The main lakes of the upstream lake chains in the Vuoksi River System are, as for the Finnish conditions, rather large. Nevertheless, the operational storage capacity of these lakes is only about one half of the storage capacity of Lake Saimaa. Of main importance for the management of the Water System are the lakes Saimaa, Pielinen and Kallavesi (Table 9).

Exceptional floods are normally multiannual, which has to be taken into account when examining the operational possibilities of the headwater lakes. Because of the limited storage capacity of the upstream lakes, it is not practical to use them for flood control in benefit of Lake Saimaa in the first year. If an extraordinary flood is threatening, first a flood release from Lake Saimaa has to be started as early as possible. An antecedent flood discharge of two months means a 10—15 cm decrease in flood level.

Table 9. The storage capacity of upstream lakes in relation to Lake Saimaa.

	The change in the water level of upper lakes[1] cm	Effect on the surface elevation of lake Saimaa cm
Pielinen	100	22
Kallavesi	50	10
Unnukka	20	approx. 0.5
Höytiäinen	20	1
Koitere	50	2

[1] The estimated storage capacity in the upper lakes

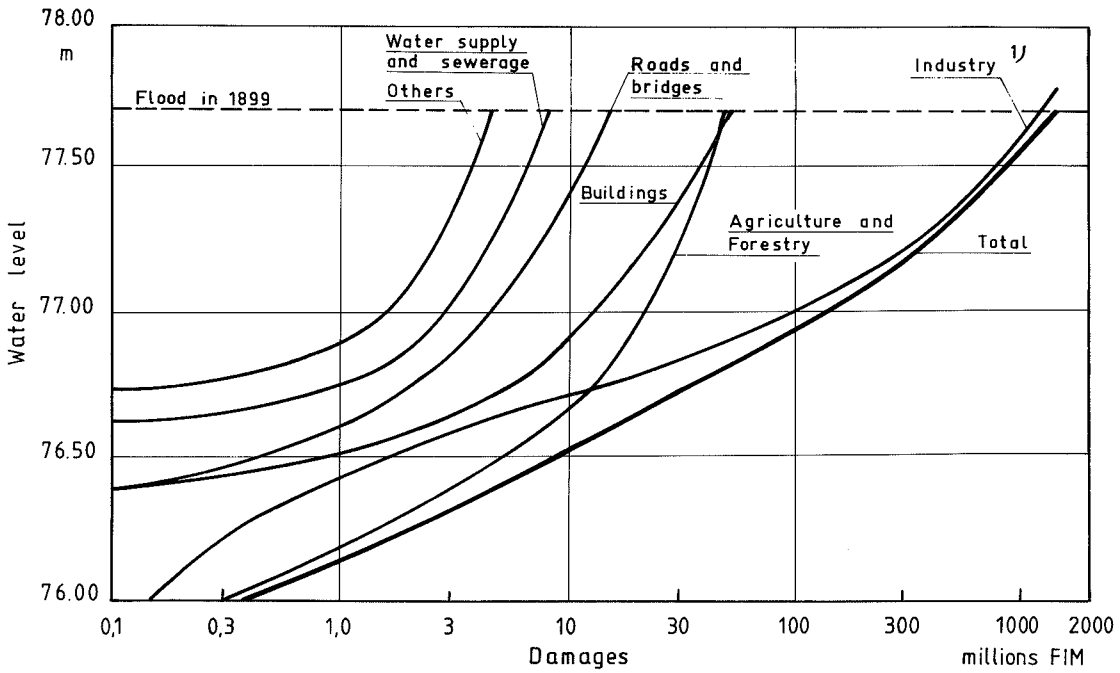

Fig. 5. The flood damages of Lake Saimaa as a function of water level. 1) Material and production costs during 180 days.

Because of the limited storage volumes compared with that of Lake Saimaa, the upstream lakes should be used as a last reserve. By storing water in these lakes during the winter of the second year an extra 20—30 cm drop in the flood stage of Lake Saimaa can be achieved. The main benefit in using the upstream lakes is gained if their capacity is used to keep the water level of Lake Saimaa below NN + 76.50 m before the melting season. Otherwise the flood risk in summer will become too high.

6 CONCLUSIONS

It can be concluded from the verification calculations, that the multireservoir regulation model can be used to simulate water resources system behaviour in various hydrological conditions. The model also allows one to study the effects of different operational alternatives and to get a good knowledge of the River System's functioning.

The model has been used for studying the flood control possibilities of Lake Saimaa and the Vuoksi River. Preliminary results show that floods can be best controlled by regulating Lake Saimaa. The upstream lakes are of minor importance because of their limited storage capacity. In severe flood situations they, however, may be valuable tools in minimizing the damages. The preliminary analysis has shown that correlations of the lake inflows for May, June, and July with total inflow for a flood period are sufficiently close, allowing one to use probabilistic methods to forecast inflow for the given months.

When developing the operational rules juridical and ecological considerations have also to be taken into account and that is why an action plan for flood control of the Vuoksi River Basin is under preparation.

REFERENCES

Bazaraa, M., Jarvis, J. 1977. Linear programming and network, 565 p.

Castren, V. 1961. Vesistöjen säännöstelytekniikka, Technical University, Helsinki.

Gürer, I. 1974. Longterm forecasting of seasonal inflows to Lake Pielinen, Aqua Fennica, Vol 4, Helsinki.

Korenistov, D.V., Kritskii, S.N., and Menkel, M.E. 1972. Problems of the Theory of Runoff Regulation. In: Problems of Investigation and Use of Water Resources, Nauka, Moscow.

Kuusisto, E. 1980. Conceptual Modelling of inflow into Lake Suur-Saimaa from the Surrounding Watersheds, Publications of the Water Research Institute n:o 39, Helsinki.

Kritskii, S.N., and Menkel, M.F. 1952. Water Resources Calculations, Hydrometeoizdat, Leningrad.

Velikanov, A.L., Korobova, D.N., and Poizner, V.I. 1983. Modelling Processes of Water Resources Systems Functioning, Nauka, Moscow.

A network flow analysis of water allocation decisions in a river system and their effect on estuarine ecology. Techn. Rep. 1978. Center for research in water resources, The University of Texas, 123 p.

SNOW COVER AND SNOWMELT RUNOFF MODEL IN THE FOREST ZONE

Juri Motovilov[1] & Bertel Vehviläinen[2]

MOTOVILOV, J. & VEHVILÄINEN, B. 1989. Snow cover and snowmelt runoff model in the forest zone. Publications of the Water and Environment Research Institute, National Board of Waters and the Environment, Finland, No. 3

Conditions of snowmelt runoff formation are similar in the watersheds of Finland and in the north-western part of the USSR forest zone. In operative hydrological practice of the Finnish National Board of Waters and the Environment a modification of the conceptual model HBV-3 is used for calculations and forecasts of spring-flood hydrograph. Within the framework of Soviet-Finnish scientific co-operation investigations are carried out to improve this version, so that it could later be used for the evaluation of the influence of man-induced factors on the runoff in forest watersheds. At the first stage model blocks, describing snow cover formation and snow melting are improved. The paper presents the main model algorithms and the results of its testing in one of Finnish watersheds.

Index words: snowmelt, snow, runoff, hydrological model

[1] Water Problems Institute, USSR Academy of Sciences, Moscow, USSR
[2] Hydrological Office, National Board of Waters and the Environment, Helsinki, Finland

1 GENERAL STRUCTURE OF THE MODEL

The HBV-model (Bergström 1976) contains a simplified description of the following processes: snow cover formation and snow melting, infiltration and accumulation of meltwater in the soil in the aeration zone, formation of surface, subsurface and groundwater runoff (Fig. 1).

1.1 Precipitation

Phase composition of precipitation was determined by the daily average air temperature (T). It was assumed, that at $T < TMIN$ only snow falls, at $T > TMAX$ — only rain and within the interval $TMAX > T > TMIN$ both snow and rain fall, and their correlation being determined by linear function on air temperature. TMIN and TMAX values

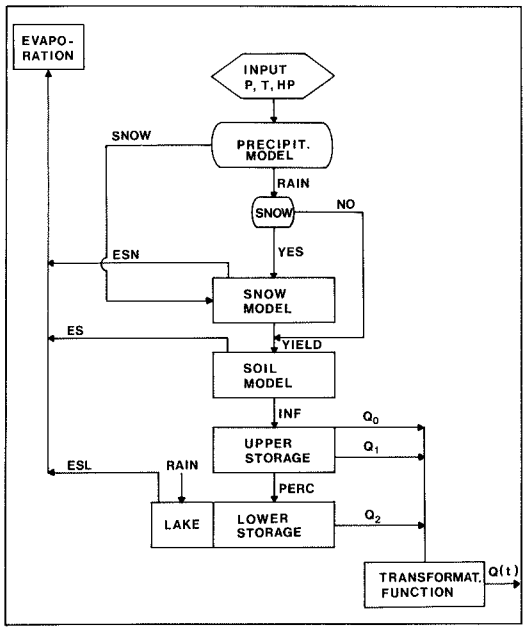

Figure 1. General structure of the runoff model.

can be taken from meteorological observation data or determined during the calibration of model parameters. In order to account the errors in measured precipitations arising from evaporation, blowing off from rain gauge and retention on crowns of forest, the amount of snow precipitation was multiplied by a specific correction coefficient 1.3 for rainfall this coefficient was equal to 1.1.

1.2 Snow cover

In the HBV-3 version used in Finland snow water equivalent was calculated by summing the amounts of snow precipitation. A method of temperature index is used to calculate snow melting. The model block, describing snow cover formation and snow melting was changed in order to improve it and will be presented in detail below.

1.3 Soil moisture storage (MVS)

Soil moisture storage in the aeration zone is determined from balance equation

$$\frac{d\,MVS(t)}{dt} = YIELD(t) - ES(t) - INF(t) \quad (1)$$

where

$$ES(t) = EP(t)\frac{MVS(t)}{LP};$$

$$INF(t) = YIELD(t)\frac{MVS(t)^{x}}{FC};$$

YIELD is the intensity of inflow of meltwater on the watershed surface; ES is evaporation intensity; INF is the intensity of water inflow into the upper soil zone (this zone may be regarded as the volume of non-capillary macro-pores in aeration zone, where subsurface flow can be generated);

EP is potential evaporation; LP is soil moisture content after which evaporation achieves its maximum; FC is the maximum soil moisture storage. The physical sense of this value is close to that of soil moisture storage under field capacity; x is a parameter; t is time.

1.4 Transformation model for runoff

1.4.1 Upper zone

Water storage in the upper zone (SUZ) (Fig. 2) is calculated according to:

$$\frac{d\,SUZ(t)}{dt} = INF(t) - Q_o(t) - Q_1(t) - PERC \quad (2)$$

where $Q_1(t) = K_1\,SUZ(t)$;

$Q_o(t) = K_o\,UZ(t)$;

$$UZ(t) = \begin{cases} SUZ(t) - LUZ & \text{if } SUZ(t) > LUZ, \\ 0 & \text{if } SUZ(t) < LUZ; \end{cases}$$

PERC is the intensity of water inflow to the lower zone; K_1, K_o are parameters.

Physical sense of Q_1 value is close to that of subsurface runoff. LUZ can be regarded as the maximum volume of noncapillary macropores in aeration zone, after these macropores are filled begins the fast flow Q_o.

1.4.2 Lower zone

The balance equation for the lower storage is as follows (Fig. 3):

$$\frac{d\,SLZ(t)}{dt} = PERC - Q_2(t) \quad (3)$$

where $Q_2 = K_2\,SLZ(t)$ is groundwater runoff.

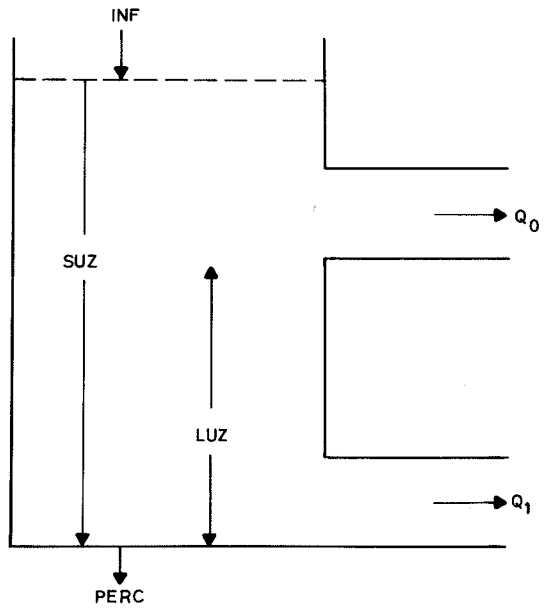

Figure 2. Upper zone.

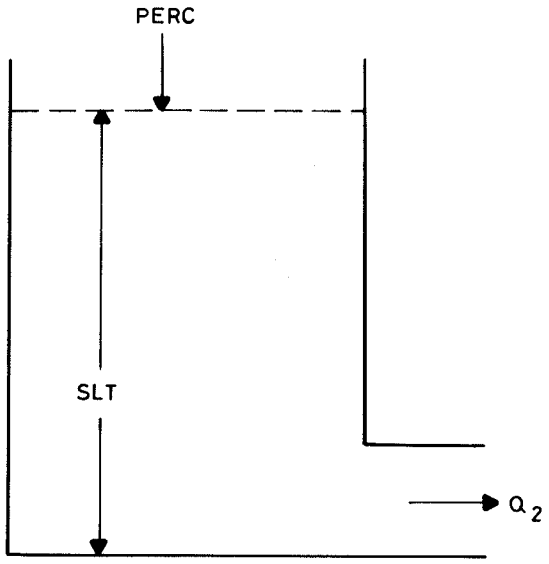

Figure 3. Lower zone.

1.4.3 River runoff

Water discharge in the outlet point in the basin Q is calculated as

$$Q(t) = KR\, Q_3(t) + (1\text{-}KR)\, Q(t-t) - Q_{min} + Q_{min} \quad (4)$$

where $Q_3 = Q_o + Q_1 + Q_2$; Q_{min} is the minimum water discharge; KR is a parameter.

2 SNOW COVER DURING ITS FORMATION AND SNOW MELTING

Snow cover characteristics undergo temporal variations, caused by precipitation, snow melting, freezing of meltwater in snow and snow compaction.

2.1 Account of precipitation

If snowfall occurs, the depth of snow cover H increases by H_p for time interval t, and

$$H_p = \frac{PSN\ RW}{RN} \quad (5)$$

where PSN is layer of snow, fallen during t period (in water equivalent); RN is density of new snow; RW is density of water.

The average snow density (DSN) in this case is calculated using the condition of mass conservation.

$$DSN = \frac{DSN'\ H' + H\ RN}{H' + H_p} \quad (6)$$

Here and below a touch indicates snow characteristics at the moment of time (t− t), disregard of the process under consideration (in this case H' is depth of snow before snowfall at the moment t − t).

If rainfall occurs, the part of rain (PLIQ) can be retained in snow under the influence of capillary-sorption forces of snow. We assumed, that if the precipitated rain cannot fill the whole snow layer, so that its maximum water-holding capacity is achieved, all the rain is retained by snow.

Else surplus rain water flows into the soil surface (water yield of snow is observed). This assumption can be expressed in a mathematical form:

$$W = \begin{cases} (W'H + PLIQ)/H & \text{if } PLIQ < (WC - W')H \\ WC & \text{if } PLIQ \geq (WC - W')H; \end{cases} \quad (7)$$

$$YIELD = \begin{cases} 0 & \text{if } PLIQ \leq (WC - W')H; \\ PLIQ - (WC - W')H & \\ & \text{if } PLIQ > (WC - W')H \end{cases}$$

$$DSN = DSN' + (W - W')\ RW$$

where W is snow moisture content (volumetric content of liquid water per unity volume of snow), WC is maximum water-holding capacity of snow (also in volumetric units).

2.2 Snow melting

Changes in snow characteristics during its melting are calculated by the following formulaes:

$$H_T = \frac{MELT\,RW}{DSN' - W'RW};$$

$$WM = \frac{W'H' + MELT}{H' - H_T}; \qquad (8)$$

$$W = \begin{cases} WM, & \text{if } WM < WC; \\ WC, & \text{if } WM \geq WC; \end{cases}$$

$$DSN = DSN' - W'\ RW + W\ RW$$

$$YIELD = \begin{cases} Q, & \text{if } WM < WC; \\ (WM - WC)(H' - H_T) & \text{if } WM \geq WC; \end{cases}$$

Here MELT is a layer of snow, melted at the Δt interval (expressed as water equivalent).

2.3 Freezing of meltwater in snow

The maximum possible amount of water, that can freeze for the Δt period (FRMAX) is calculated for the heat exchange conditions at the snow-atmosphere interface. The actual layer of frozen water FROST and residual moisture content in snow is calculated by

$$FROST = \begin{cases} FRMAX, & \text{if } FRMAX < W'H; \\ W'H, & \text{if } FRMAX \geq W'H; \\ 0, & \text{if } W' = 0; \end{cases} \qquad (9)$$

$$W = W' - FROST/H$$

2.4 Evaporation of snow

The change of snow depth during its evaporation is calculated as

$$H_E = \frac{ESN\,RW}{DSN} \qquad (10)$$

where ESN is a layer of snow, evaporated during t period (in water equivalent).

2.5 Compaction of snow

For the description of snow compaction and settling under the influence of wind loading and gravitation forces the following empirical equation is used:

$$DSN = \qquad (11)$$
$$C\,(DSN')^2\,H'\exp\,(C_2\,T_s - C_3)\,DSN')\Delta t + DSN'$$

as well as the balance equations

$$H_c = \frac{DSN'H'}{DSN};$$

$$W = \frac{W'(H - H')}{H} + W'; \qquad (12)$$

where T_s is the temperature of the snow, C a parameter, C_2 and C_3 are empirical constants.

2.6 Depth of snow

The resulting of snow cover depth at the t moment of time is determined as

$$H = H' + H_p - H_T - H_E - H_c. \qquad (13)$$

3 PHASE TRANSFORMATIONS OF WATER IN SNOW COVER

Heat flux at the snow surface is calculated using the method of energy balance, suggested by Kuzmin (1961):

$$RTOT = RSN + RLN + RSEN + RLAT + RP, \qquad (14)$$

where RTOT is a total flux of heat to the snow surface; RSN is a flux of short-wave solar radiation penetrating into the snow; RLN is the effective long-wave radiation; RSEN is sensible turbulent heat flux; RLAT is a latent heat flux; RD is a heat flux with liquid precipitation.

3.1 Short-wave solar radiation

The short wave radiation (wave length less than 3 μ) comes originally from the sun, but a part comes as a diffused component after multiply dispersed from air molecules and reflected from clouds and terrain. Heavy cloud cover can reduce the short

wave radiation to one quarter of the clear-sky value.

A large amount of incoming short wave radiation is reflected by snow cover. This portion of incoming short wave radiation, called albedo, is dependant on the wave length, the geometry of the radiation and especially on the snow structure. New snow reflects over 80 per cent whereas coarse-grained old snow reflects only 30—40 per cent of the incoming short wave radiation.

Short-wave solar radiation is calculated by equations:

$$RSN = RS\ (1\text{-}A)\ CF,$$
$$CF = 1 - F_1(1 - (1 - F)^2)^{1/2} \quad (15)$$

where RS is measured incoming short-wave radiation; A is albedo; CF is a coefficient of penetrating of short-wave radiation through tree crowns; F_1 is the parameter, introduced to take into account the type of forest; F is the forest cover density.

Snow cover albedo is calculated as (Kuchment et al. 1983):

$$A = CA - DSN \quad (16)$$

where CA is a parameter.

3.2 Effective long-wave radiation

The most part of the downward long-wave radiation comes from the lower 100 m of the atmosphere and of that 2 per cent is emitted by ozone, 17 per cent by carbon dioxide and 81 per cent by water vapour after Geiger (1961). Thus variation of downward long-wave radiation is mainly dependant on the variation of air moisture and air temperature in the 100 m layer of atmosphere above ground.
The effective long-wave radiation is calculated by:

$$RLN = E\delta\ (T + TKEL)^4\ F + (1 - F)(a + b\ e_a) - (T_s + TKEL) \quad (17)$$

where T_s is snow surface temperature, e_a is the pressure of water vapour of air, E is emissivity in the longwave portion of the energy spectrum (E = 0.99), δ is the Stefan-Boltzman constant, TKEL = 273 °K, a and b are constants.

3.3 Sensible heat transfer

Sensible heat exchange is the product of turbulent exchange processes of heat in the layer of the first two three meters above snow surface. This turbulent heat flux can be measured directly by eddy correlation techniques, which requires sophisticated instrumentation.

A more common method is to evaluate sensible heat exchange on the basis of wind and temperature profiles above the snow surface (Prandtl, 1932):

$$RSEN = -C_a\ D_a\ K_h\ dT_{pot/dz} \quad (18)$$

where C_a = specific heat of air, kJ kg °C^{-1}
D_a = air density, kJ kg^{-1} m^3
K_h = eddy diffusivity for convective energy transfer, m^2 s^{-1}
T_{pot} = potential temperature i.e. temperature at the surface pressure

In practice the eddy diffussivit is calculated from wind profile and assuming that the eddy diffusivity for convective heat transfer K_h equals eddy diffussivity for momentum K_m, which is usually valid during snowmelt (Anderson, 1976).

This method of profiles is valid only for open areas, where well-defined wind and temperature profiles can exist. In forested area the vegetation prevents the formation of welldefined wind and temperature profiles 2—3 meters above snow. Therefore it is reasonable to use simplified equations for sensible heat exchange in the forested basins. These equations are usually the form:

$$RSEN = CS\ U\ (T - T_{snow}) \quad (19)$$

where CS = bulk transfer coefficient for sensible heat exchange kJ (m^{-3} °C^{-1}) the value of which varies from 0.001 to 0.015 (Male et al. 1981)
U = wind speed (m s^{-1})

The value of bulk transfer coefficients are usually averages over relative long periods and equation 84 should not be applied over intervals of less than 24 h at least with the presented coefficient values.

3.4 Latent heat transfer

Turbulent mixing of the air layers is the main process causing heat and moisture transfer above snow surface. Because the origin of these two exchange processes is the same they also occur simultaneously. Sensible and latent heat exchange needs the

gradient of temperature and moisture on one hand and wind on the other hand to exist. Moisture and temperature gradients are developed due to the energy supply of short wave and long wave radiation. Wind tends to eliminate gradients increasing simultaneously turbulent heat absorption/intake and moisture evaporation/condensation. In the absence of wind heat and moisture transfer ceases although gradient exist· there is no turbulent transport process. On the other hand wind can eliminate weak gradients easily and this ceases again the transfer of heat and moisture.

The same method of profiles or gradients, that is used for sensible heat exchange is also valid for latent heat exchange (Prandtl 1932):

$$RLAT = -HV\ D_a\ K_e\ de_a/dz \qquad (20)$$

where HV = heat of vaporization, 335 kJ kg^{-1}
K_e = eddy diffusivity of latent energy transfer $m^2\ s^{-1}$)
e_a = air moisture, mb

The eddy diffusivity of momentum K_m is calculated first from wind profile. With assumption that K_e/K_m is unity during snowmelt latent heat exchange can be evaluated based on measurements on two levels.

The same reasons, absence of well-defined wind and moisture profiles near surfacxe, which led to the use of simplified equations of sensible heat in forested areas are valid also for latent heat exchange. For the simulation of latent heat exchange in forested basins equation is used as for sensible heat:

$$RLAT = CL\ U\ (e_a - e_s) \qquad (21)$$

where CL = bulk transfer coefficient for latent heat exchange, kJ m^{-3} mb^{-1}
e_s = vapour pressure on the snow surface, mb
e_a = vapour pressure in air over snow, mb

The values of CL vary from 0.002 to 0.025 kJ m^{-3} mb according to Male et al. (1981).

3.5 Heat flux by rain

With precipitation heat it is considered the heat or energy, that is delivered to a snowpack, when water from precipitation reaches the temperature of snowpack and, if the temperature is under 0 °C, freezes. In the first case without freezing the energy supply to the snowpack, RP, is:

$$RP = D_w\ C_w\ (T_p - T)\ P/1000 \qquad (22)$$

where D_w = density of water, kg m^{-3}
C_w = specific heat of water, kJ kg^{-1} $°C^{-1}$
T_p = temperature of rain, °C
P = precipitation, mm d^{-1}

The energy supply by this process is quite small compared to other components of energy balance equation.

In the case all liquid precipitation is freezed in snowpack the energy supply from liquid precipitation becomes important compared to other energy balance terms. The latent heat of the fusion of water is 335 kJ kg^{-1}. This is possible only in the beginning of snowmelt, when the temperature of snowpack is below 0 °C.

The energy supply from 1 mm of rain at 5 °C air temperature when temperature of snowpack is −10 °C is about 6 J cm^{-2} after equation 22 and when the water is freezed the additional energy supply to the snowpack is 34 J cm^{-2}.

With abundant rainfall on snow the heat from liquid precipitation is distributed rapidly into the whole snowpack. Rainfall may change the structure of snow very quickly compared to normal melting process.

3.6 Snow melting and freezing of meltwater in snow

Snowpack during melting period is characterized by the following values: TS = 0 °C; ES = 6.11 mb. Substituting these values into formulae (17) — (20) we can determine RTOT. The amount of snow melted or water frozen in snow is determined from the relations:

$$MELT = \begin{cases} RTOT/CM, & \text{if } RTOT > 0; \\ 0, & \text{if } RTOT \leq 0; \end{cases} \qquad (23)$$

$$FRMAX = \begin{cases} 0, & \text{if } RTOT > 0; \\ -RTOT/CM, & \text{if } RTOT \leq 0; \end{cases}$$

where CM is the heat of fusion of ice.

4 TESTING OF THE MODEL

Calibration of parameters and testing of the model were carried out in the basin of the Tujuoja river (Finland).

Tujuoja is a small experimental basin near western coast of Finland 64 °N, 25 °E. The area is 20.6 km^2 of which 82 % is forest (canopy density 30 %), 12 % field, 4 % bog and 2 % urban area. There are no lakes in the area and the mean slope is 2.3 %.

4.1 Calibration of parameters

The model parameters were calibrated on the basis of observed data of water discharges and the characteristics of snow cover during 1977—1981. The Rosenbrock optimization procedure was used for the calibration of the parameters with a quality criteria:

$$R^2 = \frac{(Q_r - \bar{Q}_r)^2 - (Q_c - Q_r)^2}{(Q_r - \bar{Q}_r)^2} \quad (24)$$

where Q_c is the calculated value, Q_R is the observed value, $\bar{Q}_r$ is the average from observed values.

At the first stage parameters of the submodel, describing snow cover, were calibrated using measured snow cover characteristics (depth, density and water equivalent of snow). Calculation showed, that the best agreement between calculated and observed values is achieved, when parameters are calibrated over snow depth. Calibration over the values of snow density or its water equivalent has considerably worsend results.

This is assumed to be connected mainly with low accuracy of measuring snow density.

At the second stage model parameters describing soil characteristics and storage zone were calibrated by measuring water discharge in the outlet point.

At the third stage parameters of blocks describing energy balance and snow cover formation were adjusted against measured water discharge.

4.2 Verification of the model

Model parameters, received as a result of calibration were used in test calculations for the Tujuoja river basin in 1970—1976. Table 1 contains the values of quality criterion for calibration and verification of the model.

Table 1. Quality criterion for calibration and verification of snowmelt runoff model.

Characteristics	R^2 Calibration	R^2 Verification
Depth of snow	0.850	0.618
Density of snow	0.525	0.201
Water equivalent	0.807	0.620
Runoff	0.850	0.710

Figures 4 and 5 present some results of model calibration and verification.

SUMMARY

The aim of this study was to develop a physically based snowcover model for simulation of snow accumulation and snow melt, which can be used for operational purposes in large river basins with minimum input data on daily basis. The physically based model should also be better than the common degree-day snow models used normally in operational catchment hydrology. This criterion is not yet achieved with this model to be presented or with any other physical snowcover model. Anyway physically based snowcover model gives a lot of information of the different processes included in snow accumulation and snowmelt phenomenon, which can be usable in developing simpler snow models. Also physically based snow models can simulate quite accurately different snow characteristics as snow density and depth, which can be used in some other studies as soil frost simulation or in calculation of snow albedo.

REFERENCES

Anderson, E.A. 1976. A point energy and mass balance model of a snowcover. NOAA Tech.Rep. NWS-19, U.S.Dept. Commer., Washington, D.C.

Bergström, S. 1976. Development and application of a conceptual runoff model for Scandinavian catchments. SMHI, Nr RHO 7, Norrköping.

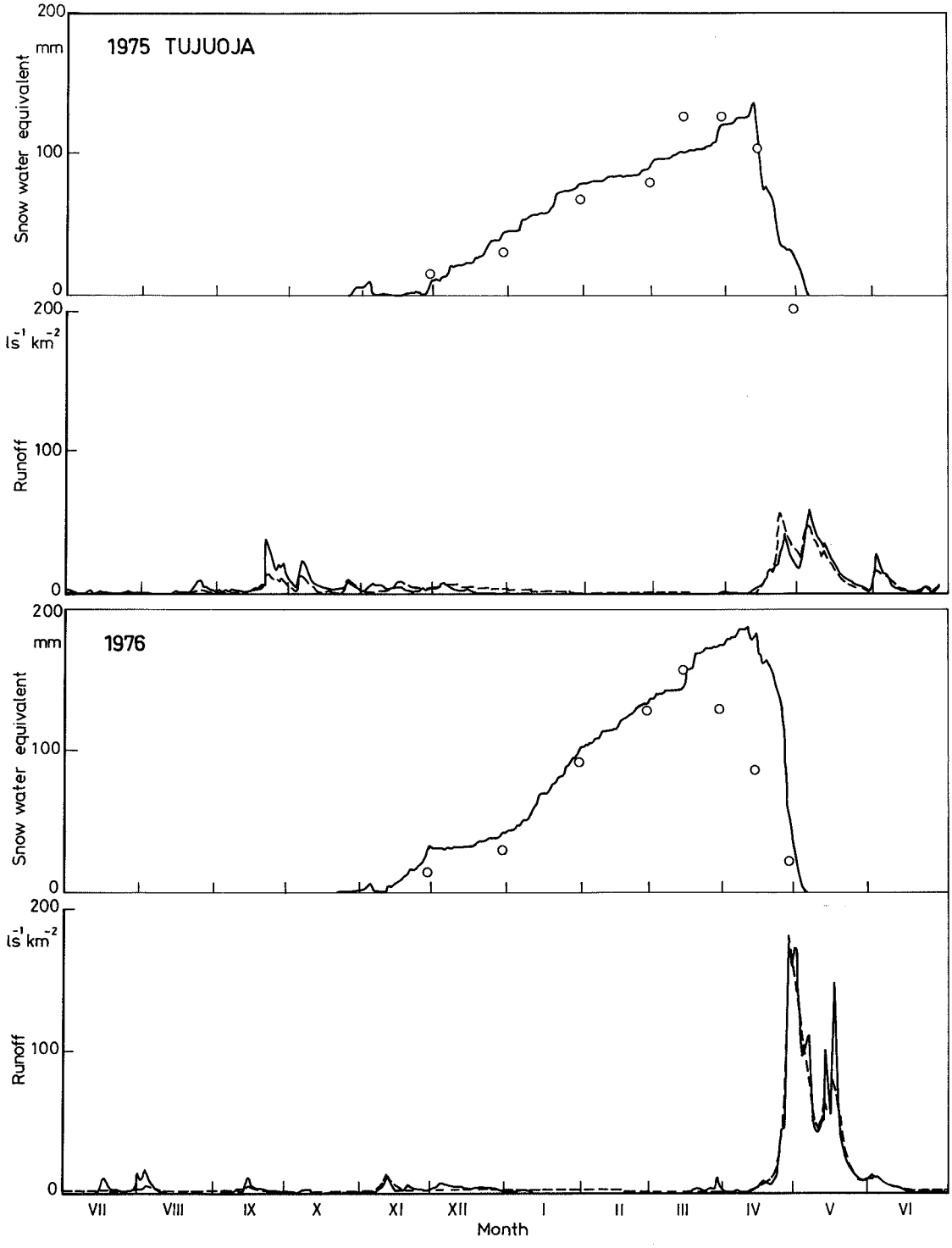

Figure 4. Simulation of water equivalent and runoff in the Tujuoja basin in the winters 1975—1977. Observed water equivalent is marked by (o) and observed runoff is full line.

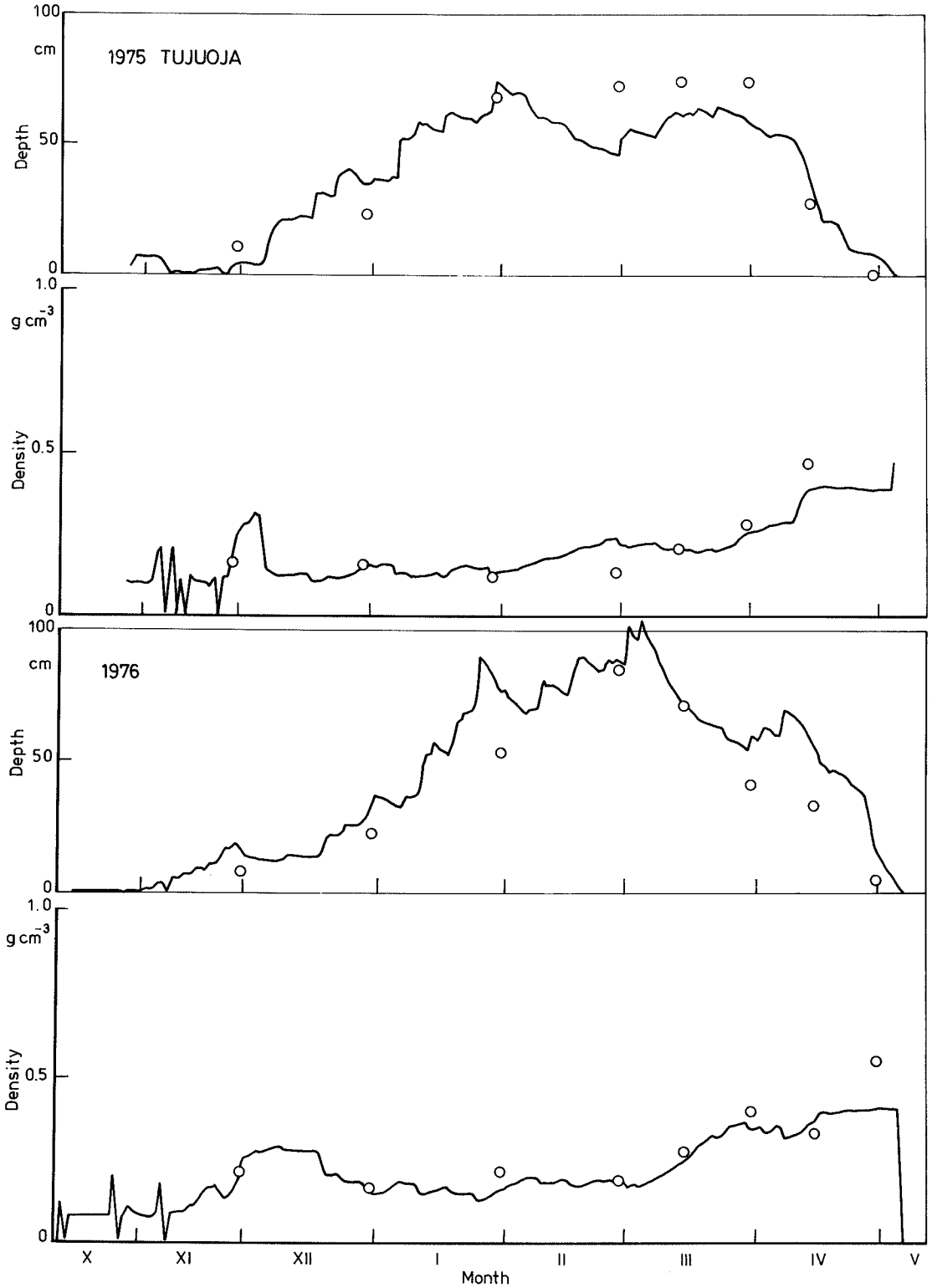

Figure 5. Simulation of the depth and density of snow in Tujuoja basin in the winters 1975—1977. Observed values are marked by (o).

Geiger, R. 1961. Das Klima der bodennahen Luftschicht (The Climate Near the Ground). (English Transl. by Scripta Technica Inc., Harvard University Press, Cambridge, Mass.)
Kuchment, L.S., Demidov, V.N. & Motovilov, Ju. 1983. Forming of river runoff (a physically based model). Moscow.
Kuzmin, P.P. 1961. Melting of snow cover. Leningrad.
Male, D.H. & Gray, D.M. 1981. Snowcover ablation and runoff. Handbook of Snow. Pergamon Press.
Prandtl, L. 1932. Meteorologische Anwendung der Strömungslehre. Beitr. Phys. d. freien Atmos., Vol. 19, p. 188—202.
Vehviläinen, B. 1986. Modelling and forecastging snowmelt floods for operational forecasting in Finland. IAHS Publ. No. 155. Budapest.

LIST OF SYMBOLS

DSN	= snow density	kg mg^3
EP	= potential evaporation	cm d^{-1}
ES	= actual evaporation	cm d^{-1}
ESN	= snow evaporation	cm d^{-1}
FC	= maximum value of soil moisture storage	mm
FROST	= backfreezing in snowpack	cm d^{-1}
H	= snow depth	cm
INF	= water yield from soil moisture storage	mm d^{-1}
K_o	= runoff coefficient	1 d^{-1}
K_1	= runoff coefficient	1 d^{-1}
K_2	= runoff coefficient	1 d^{-1}
KR	= recession coefficient	0—1
LP	= soil moisture storage value after which the actual evaporation equals the potential evaporation	mm
MELT	= snow melt	cm d^{-1}
MVS	= soil moisture storage	mm
PERC	= water inflow to the lower zone	mm d^{-1}
PLIQ	= liquid precipitation	mm
PSN	= snow precipitation	cm
RN	= density of new snow	kg m^{-3}
RW	= density of water	kg cm^{-3}
SLZ	= water storage in the lower zone	mm
SUZ	= water storage in the upper zone	mm
T	= daily mean temperature	°C
T_s	= temperature of snow	°C
TMAX	= daily temperature over which all precipitation is liquid	°C
TMIN	= daily temperature below which all precipitation is solid	°C
W	= volumetric content of liquid water in snow	m^3 m^{-3}
WC	= maximum water-holding capacity of snow in volumetric units	m^3 m^{-3}
YIELD	= water yield from liquid precipitation and snow melt	mm d^{-1}

MODEL OF COMBINED WATER USE AND WATER DERIVATION PLANNING

Andrey Kocharian[1], Iosif Khranovich[1]

KOCHARIAN, A., KHRANOVICH, I. 1989. Model of combined water use and water derivation planning. Publication of the Water and Environment Research Institute, National Board of Waters and the Environment, Finland, No. 3.

The paper presents a flow model describing the selection of optimum parameters of water resource system elements: sources of water and pollutants, water reservoirs, reaches of rivers and canals, water users, water protection facilities. The model takes into account both water use and water quality control.

Index words: water resource system (WRS), two-stage stochastic flow model, interacting flows, variants of element's development, characteristic function of development alternatives, multiextremal task.

[1] Water Problems Institute of the USSR Academy of Sciences 13/3 Sadovo-Chernogriazskaya, 103064 Moscow USSR

1 INTRODUCTION

A water resource system (WRS) involves an assembly of interacting sources of water, reservoirs, seas and water users, connected by river and canal reaches.

A WRS coordinates water demands with available water resources. According to this function of the system, its parameters are to be coordinated in a most effective way. In this particular paper under the term "optimum" such WRS parameters and operational regimes are meant, with which national economy expenses for the desing period are minimized. Costs involve capital investments and operation and maintenance costs. Effect of water use is also accounted in them.

Considering the selection of WRS parameters it

is supposed that parameters of elements of the existing WRS (volumes of reservoirs, canal capacities and efficiency, production capacities, i.e. capacitie of enterprises — water-users and purification facilities, etc.) and probable regimes of water and pollutant entry into the system are known. Reconstruction elements and elements under construction with possible values of their parameters, received as a result of preliminary studies, are known too. Solution of this problem consists in selection of the optimum set of parameters of WRS elements among the probable ones.

It requires a great number of possible sets of elements' parametres and relevant operation regimes of the system to be compared. To solve the problem an optimization model is used, where all permissible sets of alternatives are compared. Water distribution and water quality control are analysed jointly in the suggested model. Such an approach, unlike the traditional separate analysis of quantitative and qualitative characteristics, allows all water management measures to be solved in one complex.

The system is assumed to operate in discrete time. The model takes into account random processes of water and pollutants entry and utilization, which is presented by a finite set Ω of characteristic realizations of conditions ω.

2 MODELS OF WRS ELEMENTS

A WRS is presented by a network $\Gamma(J,S)$, the configuration of which corresponds to a diagram WRS presentation. In the network $\Gamma(J, S)$ all the assumed WRS elements, existing or possible, are represented. Elements of this network have their own characteristics, their interaction is produced by flow movement, corresponding to water and admixture flows in the simulated system.

For any WRS element a finite set of possible development alternatives are singled out. Each of them is characterised by a set of elements' parameters.

In the model every version of WRS elements' development is presented as an operational element. Operation of the z-th element according to teh z_α-th alternative of development is described by a characteristic function of the version $\eta_{z\alpha} = 1$, if the z_α-th alternative is accepted; $\eta_{z\alpha} = 0$, if the z_α-th version is not accepted. As a WRS element can operate according to one version of the finite sets a_z, characteristic functions of elements' development alternatives are linked by:

$$\eta_{z\alpha} \in \{0; 1\}, \sum_{z_\alpha \in a_z} \eta_\alpha = 1 \tag{1}$$

River and canal reaches and water users, except those using water from reservoirs without its divertion and considered as a single whole together with reservoirs, are depicted by Γ (J,S) arcs with gain and retardation.

The flow $q^{\omega}_{s\alpha}$ at the beginning of the s_α-th arc corresponds to the s_α-th variant of the set a_s of possible development variants of the s-th user under ω stochastic conditions, is connected with the flow $q^{\kappa\omega}_{s\alpha}$ at the end of this arc by the inequality:

$$q^{\kappa\omega}_{s\alpha t} = K^{\omega}_{s\alpha t}\, q^{\omega}_{s\alpha,\, t-\theta} \tag{2}$$

without non-negative retardation $\theta^{\omega}_{s\alpha t}$ and an amplification factor, having the meaning of a ratio of water, returned by the user, to the amount of water, allocated to the user. Its values are within the range $1 \geq K^{\omega}_{s\alpha t} \geq 0$.

In the model users' requirements to water resources quantity and water consumption restrictions cause the appearence of sets of possible values of arc flows:

$$\underline{q}^{\omega}_{s\alpha t} \leq q^{\omega}_{s\alpha t} \leq \bar{q}^{\omega}_{s\alpha t} \tag{3}$$

Water sources with uncontrolled consumption (natural river runoff) in the model are presented by sources of prescribed intensities b^{ω}_{it} located at $i \in J$.

Water sources with controlled consumption (presented by systems of interregional water transfer) are described by fragments of the network Γ (J, S), each having vertices, the number of which equals the number of versions of the source's development. Every vertex is connected with the rest of the network by outgoing arcs $s_{\alpha 1}$ and $s_{\alpha 2}$ with the gain coefficients $K^{\omega}_{s\alpha 1} = 1$, $K^{\omega}_{s\alpha 2} = 0$.

Reservoirs and seas in the model are regarded as a single whole with users, located on them. They are expressed by storages in the graph's vertices. Their supplies $Q^{\omega}_{i\alpha t}$ equal the amount of water in the reservoirs and seas. These constraints cause sets of possible values of storage supplies:

$$\underline{Q}^{\omega}_{i\alpha t} \leq Q^{\omega}_{i\alpha t} \leq \bar{Q}^{\omega}_{i\alpha t} \tag{4}$$

In the model relationship between the intensity of water losses in reservoirs and seas due to seepage and evaporation are approximated by linear ones:

$$\delta Q^{\omega}_{i\alpha t} = \gamma^{\omega}_{i\alpha t}\, Q^{\omega}_{i\alpha t} \tag{5}$$

3 POLLUTANTS AND WATER QUALITY

In addition to "basic" flows $q^{\omega}_{s\alpha t}$ and supplies $Q^{\omega}_{i\alpha t}$ expressing water storage and discharge, "additional" flows $y^{\omega}_{s\alpha lt}$ and supplies $Y^{\omega}_{i\alpha lt}$, simulating pollutants (l is the type of pollutant), are included in the model. Interaction of these flows corresponds to representation of processes of pollutant proliferation and transformation by a system of linear differential equations of the Streeter-Phelps type, (Vavilin et al. 1977).

In the elements of the network flows and supplies of pollutants of each set L_ν should meet the following requirements:

$$\sum_{l \in L_\nu} d^{\omega}_{z\alpha lt} Z^{\omega}_{z\alpha lt} \leq \beta^{\omega}_{z\alpha t} X^{\omega}_{z\alpha t}, \; z_\alpha \in R = S \cup I. \qquad (6)$$

The set of types L of pollutants are divided into subsets L_ν, which have an unempty crossing according to a limiting factor in such a way that $\bigcup_\nu L_\nu = L$, where $d^{\omega}_{z\alpha lt}$ is the value, inverse to the maximum permissible concentration $\bar{C}^{\omega}_{z\alpha lt}$ of the l-th admixture in the z_α-th element of Γ (J, S) under stochastic conditions ω; if $z_\alpha \in S$ $Z^{\omega}_{z\alpha lt}$ denotes a pollutant flow of l type in the z_α arc $y^{\omega}_{z\alpha lt}$, where $z_\alpha \in I$ $Z^{\omega}_{z\alpha lt}$ pollutant supply of l-th type in the z_α-th storage $Y^{\omega}_{z\alpha lt}$; $X^{\omega}_{z\alpha t}$ denotes a water flow $q^{\omega}_{z\alpha t}$ and supply $Q^{\omega}_{z\alpha t} \cdot \beta^{\omega}_{z\alpha t}$ is the coefficient of incomplete mixing, which is equal to the ratio of the average pollutant concentration to maximum pollutant concentration. If $z_\alpha \in S$, the conditions (6) correspond to arcs' inlets and reflect users' requirements to the quality of water, allocated to them. Requirements to the quality of water, returned to the system, are prescribed by similar conditions, imposed on the pollutant composition at arcs' outlets:

$$\sum_{l \in L_\nu} d^{\kappa\omega}_{s\alpha lt} y^{\kappa\omega}_{z\alpha lt} \leq \beta^{\kappa\omega}_{s\alpha t} q^{\kappa\omega}_{s\alpha t}, \; s_\alpha \in S. \qquad (7)$$

Moreover, the values of pollutant flows and supplies have lower limits:

$$Z^{\omega}_{z\alpha lt} \geq \underline{Z}^{\omega}_{z\alpha lt}, \; y^{\kappa\omega}_{s\alpha lt} \geq \underline{y}^{\kappa\omega}_{s\alpha lt}, \; z_\alpha \in R, \; s_\alpha \in S \qquad (8)$$

The constants $d^{\omega}_{z\alpha lt}$, $d^{\kappa\omega}_{s\alpha lt}$, $\underline{Z}^{\omega}_{z\alpha lt}$, $\underline{y}^{\kappa\omega}_{s\alpha lt}$ are non-negative. It should be noted, that conditions (6) and (7) impose stricter requirements on the pollutant composition than non-excess of pollutant concentration $C^{\omega}_{z\alpha lt} = Z^{\omega}_{z\alpha lt}/X^{\omega}_{z\alpha t}$ and $C^{\kappa\omega}_{s\alpha lt} = y^{\kappa\omega}_{s\alpha lt}/q^{\kappa\omega}_{s\alpha t}$ of all the pollutants, taken separately.

From the assumptions of complete momentary mixing and linearity of pollutant composition variations it follows that pollutant supplies in the storage satisfies the following:

$$Y^{\omega}_{i\alpha l, t+1} = \sum_{\gamma \in L} A^{\gamma l\omega}_{i\alpha t} Y^{\omega}_{i\alpha\gamma t} + h_t y^{\omega}_{i\alpha lt}, \qquad (9)$$

where $A^{\omega}_{i\alpha t} = \{A^{\gamma l\omega}_{i\alpha t}\}$, $\gamma, l \in L$ is the non-singular square matrix of substances transformation in the storage.

Solving the system of linear differential Streeter-Phelps equations a relationship is obtained between the vectors of pollutants at the inlets and outlets of the arcs, forming the set $S_I \subset S$ and representing in Γ (J, S) users without treatment facilities, river and canal reaches:

$$y^{\kappa\omega}_{s\alpha lt} = \sum_{\gamma \in L} A^{\gamma l\omega}_{s\alpha t} y^{\omega}_{s\alpha\gamma, t-\theta} \qquad (10)$$

A functional relationship of type (10) between pollutant flows at the arcs' inlets and outlets, representing users and sources with treatment facilities in the model and forming the set $S_{II} = S \setminus S_I$, is absent, since, due to operational regimes of treatment facilities, for the same value $y^{\omega}_{s\alpha lt}$ different values $y^{\kappa\omega}_{s\alpha lt}$ can be received. Pollutant flows $y^{\omega}_{s\alpha lt}$ and $y^{\kappa\omega}_{s\alpha lt}$ are interconnected by operation and maintenance costs of elements with treatment facilities.

Inevitability of receiving water with pollutants brings about a requirement of coincidence of a heterogenuous flow composition at the inlets of arcs, starting from one and the same vertex:

$$y^{\omega}_{s\alpha lt} \, q^{\omega}_{\tilde{s}\alpha t} = y^{\omega}_{\tilde{s}\alpha lt} \, q^{\omega}_{s\alpha t}, \; s_\alpha, \tilde{s}_\alpha \in S_i^- . \qquad (11)$$

4 CONTINUITY EQUATIONS

In the WRS water and pollutant distribution, subjected to the mass conservation law, in accordance with water and pollutant flows in Γ (J, S), meet the following system of continuity equations:

$$\sum_{i\alpha \in a_i} [Q^{\omega}_{i\alpha, t+1} - Q^{\omega}_{i\alpha t}] = h_t \cdot \sum_{i\alpha \in a_i} q^{\omega}_{i\alpha t} =$$

$$= h_t \left[\sum_{s\alpha \in S_i^+} q^{\kappa\omega}_{s\alpha t} - \sum_{s\alpha \in S_i^-} q^{\omega}_{s\alpha t} - \sum_{i\alpha \in a_i} \delta Q^{\omega}_{i\alpha t} + 6^{\omega}_{it} \right] \qquad (12)$$

$$\sum_{i\alpha \in a_i} y^{\omega}_{i\alpha lt} = \sum_{s\alpha \in S_i^+} y^{\kappa\omega}_{s\alpha lt} - \sum_{s\alpha \in S_i^-} y^{\omega}_{s\alpha lt} + 6^{\omega}_{ilt}, \qquad (13)$$

where S_i^+ is the set of arcs, coming into the i-th vertex; S_i^-, the set of arcs, outgoing from the i-th vertex; 6^{ω}_{ilt} is the pollutant flow of the l-th type, coming into the i-th vertex under the conditions ω.

5 RESOURCE CONSTRAINTS

The suggested model involves conditions, reflecting constraints of labour, financial and other resources and tasks on production targets, produced by water users; those conditions include constraints on the resources, connected with the WRS development and operation.

Resource constraints on development are represented by the system of inequalities

$$\sum_{z\alpha\epsilon R} m^{d}_{z\alpha}\,\eta_{z\alpha} \le M^{d},\ d \epsilon D_{I}, \qquad (14)$$

where M^{d} is the total amount of the d-type resource, which can be allocated for the WRS development (capital investments, building materials, etc); D_I is the set of resource types taken into account, used in the WRS elements' construction and reconstruction; $m^{\alpha}_{z\alpha}$ is the amount of d-type resource, necessary for the introduction of the α-version of development of the z-th element of the WRS.

In operating WRS restricted stored and unstored resource are used. Stored resources involve utilized raw materials and reagents for water treatment; unstored resources are labour resources, electric power, resources of irrigation facilities, etc.

Employment conditions of stored resources cover the whole design period and are described by the system of inequalities:

$$\sum_{t\epsilon[To,\,T]}\Big[\sum_{z\alpha\epsilon R}\varphi^{d\omega}_{z\alpha t}\,(X^{\omega}_{z\alpha t},\,U^{d\omega}_{z\alpha t}) + \sum_{s\alpha\epsilon S_{II}}\varphi^{\kappa d\omega}_{s\alpha t}\,(X^{\kappa\omega}_{s\alpha t},\,U^{\kappa d\omega}_{s\alpha t})\Big] \le M^{d\omega},\ d \epsilon D_{II}. \qquad (15)$$

Here $M^{d\omega}$ and d have the same meaning as in (14); D_{II} is the the set of stored resources, $\varphi^{d\omega}_{z\alpha t}$ and $\varphi^{\kappa d\omega}_{z\alpha t}$ relationships of the resource magnitude being utilized and water quality and quality in the element (φ) and returned into the system (φ^{κ}); $U^{d\omega}_{z\alpha t} = \sum_{l\epsilon L}\delta^{dwl}_{z\alpha t}\,y^{\omega}_{z\alpha lt}$ and $U^{\kappa d}_{s\alpha t} = \sum_{l\epsilon L}\delta^{\kappa dwl}_{s\alpha t}\,y^{\kappa\omega}_{s\alpha lt}$ pollutant complexes in the element and returned into the WRS; $\delta^{dwl}_{z\alpha t}$ and $\delta^{\kappa dwl}_{s\alpha t}$ are non-negative numbers, reflecting the significance of the l-th pollutant in a complex.

Functions $\varphi^{d\omega}_{z\alpha t}$ and $\varphi^{\kappa d\omega}_{s\alpha t}$ are convex in each of the variables $X^{\omega}_{z\alpha t}$, $U^{d\omega}_{z\alpha t}$ and $x^{\kappa\omega}_{s\alpha t}$, $u^{\kappa d\omega}_{s\alpha t}$; they are non-convex in their totality, (Priazhunskaya et al., 1978).

Unstored resources are used only in time intervals, when they are not singled out. Conditions of their utilization correspond to these time intervals and are as follows:

$$\sum_{z\alpha\epsilon R}\varphi^{d\omega}_{z\alpha t}\,(X^{\omega}_{z\alpha t},\,U^{d\omega}_{z\alpha t}) + \sum_{s\alpha\epsilon S_{II}}\varphi^{\kappa d\omega}_{s\alpha t}\,(X^{\kappa\omega}_{s\alpha t},\,U^{\kappa d\omega}_{s\alpha t}) \le M^{d\omega}_{t},\ d \epsilon D_{III}, \qquad (16)$$

where D_{III} is the set of unstored resources. Functions of consumption of unstored resources, presented in (16), have the meaning and characteristics, similar to those, presented in (15).

Conditions of achieving production targets, depending on the possifility of accumulating during the desing period, are introduced into the model in the form of (15) or (16). Besides, functions $\varphi^{d\omega}_{z\alpha t}$ have the meaning of the relationship of production targets amount of water resources quality and quantity.

6 TASK FUNCTION

The WRS development over the design period is estimated by the cost function, including expences on construction and renovation, operation and maintenance, on output, delivery, and purification of water, as well as expences, arising from the deviation of water quantity and quality from the optimum.

The functions describe the mathematical expectation of costs over the design period:

$$f_z(\eta_z,\,x_z,\,y_z) = \sum_{z\alpha\epsilon a_z}\Big[K_{z\alpha}\eta_{z\alpha} + \sum_{\omega\,\epsilon\,\Omega}\rho_{\omega}\sum_{t\,\epsilon\,[To,\,T]}\big[f^{\omega}_{z\alpha t}(x^{\omega}_{z\alpha t},\,u^{\omega}_{z\alpha t}) + f^{\kappa\omega}_{z\alpha t}(x^{\omega}_{z\alpha t},\,u^{\kappa\omega}_{z\alpha t})\big]\Big], \qquad (17)$$

where coefficients $K_{z\alpha}$ reflect constant costs independent of operational regimes $x^{\omega}_{z\alpha t}$ and $u^{\omega}_{z\alpha t}$. Functions $f^{\omega}_{z\alpha t}$ and $f^{\kappa\omega}_{z\alpha t}$ estimate variable costs, depending on $x^{\omega}_{z\alpha t}$ and $u^{\omega}_{z\alpha t}$. Components $f^{\kappa\omega}_{z\alpha t}$ are not equal to zero, only if $z_{\alpha} \epsilon S_{II}$. Functions $f^{\omega}_{z\alpha t}$ and $f^{\kappa\omega}_{z\alpha t}$ have characteristics similar to those of functions $\varphi^{d\omega}_{z\alpha t}$ and $\varphi^{\kappa d\omega}_{z\alpha t}$ i.e they are convex in each of the variables $z^{\omega}_{z\alpha t}$ and $u^{\omega}_{z\alpha t}$ and non-convex in their totality, (Priazhinskaya et al., 1978); $f^{\omega}_{z\alpha t}(0,0) = f^{\kappa\omega}_{z\alpha t}(0,0) = 0$.

7 DEVELOPMENT TASK

Determination of optimum WRS parameters and operation regimes is described by the task A of

determination of the optimum parameters and sources of the network $\Gamma(J, S)$. The task deals with the estimations of vectors η°, x°, y° with strategic components $\eta^\circ = |\eta^\circ_{z\alpha},\ z_\alpha \in R|$ and tactical components $x^\circ = |x^{\omega\circ}_{z\alpha t},\ x^{\omega\circ}_{z\alpha t};\ z_\alpha \in R,\ s_\alpha \in S_{II},\ \omega \in \Omega,$

$t \in [To, T]|$, $y^\circ = |y^{\omega\circ}_{z\alpha lt},\ y^{\kappa\omega\circ}_{s\alpha lt};\ z_\alpha \in R,\ s_\alpha \in S_{II},\ l \in L,$

$\omega \in \Omega,\ t \in [To,\ T]|$ which minimize the mathematical expectation of the WRS costs:

$$f(\eta, x, y) = \sum_{z\in R} f_z(\eta_z, x_z, y_z) = \tag{18}$$

$$= \sum_{z\in R} [K_{z\alpha}\eta_{z\alpha} + \sum_{\omega\in\Omega} \rho^\omega \sum_{t\in[To,\ T]} [f^\omega_{z\alpha t}(x^\omega_{z\alpha t}, u^\omega_{z\alpha t}) + f^{\kappa\omega}_{z\alpha t}(x^\omega_{z\alpha t}, u^{\kappa\omega}_{z\alpha t})]]$$

in the set G, formed by constraints (1)—(16). G is prescribed by the system of continuity equations of water and pollutant flows:

$$\sum_{i\alpha\in a_i} [Q^\omega_{i\alpha,\ t+1} - K^\omega_{i\alpha t} Q^\omega_{i\alpha t}] = h_t [\sum_{s\alpha\in S_i^+} K^\omega_{s\alpha t} q^\omega_{s\alpha t} - \sum_{s\alpha\in S_i^-} q^\omega_{s\alpha t} + 6^\omega_{it}], \tag{19}$$

$$\sum_{i\alpha\in a_i} [Y^\omega_{i\alpha l,\ t+1} - \sum_{\gamma\in L} A^{\gamma l\omega}_{idt}\, Y^\omega_{i\alpha lt}] =$$

$$h_t [\sum_{s\alpha\in S_i^+} y^{\kappa\omega}_{s\alpha lt} - \sum_{s\alpha\in S_i^-} y^\omega_{s\alpha lt} + 6^\omega_{ilt}],\ l \in L \tag{20}$$

by transforming equations of pollutants in arcs, depicting river and canal reaches, users and sources without treatment facilities:

$$y^{\kappa\omega}_{s\alpha lt} = \sum_{\gamma\in L} A^{\gamma l\omega}_{s\alpha t}\, y^\omega_{s\alpha\gamma,\ t-\theta},\ s\alpha \in S_I, \tag{21}$$

by equations of pollutant concentration in arcs, outgoing from one and the same vertex

$$y^\omega_{s\alpha lt}\, q^\omega_{\tilde{s}\alpha t} = y^\omega_{\tilde{s}\alpha lt}\, q^\omega_{s\alpha t},\ s, \tilde{s} \in S_i^-,\ l \in L, \tag{22}$$

upper and lower limits of flow magnitudes in arcs and storage supplies as well as amounts and compositions of impurities (pollutants) in arcs and storages:

$$\eta_{z\alpha}\, \underline{x}^\omega_{z\alpha t} \le x^\omega_{z\alpha t} \le \eta_{z\alpha}\, \bar{x}^\omega_{z\alpha t},\ x_\alpha \in R,$$

$$\sum_{l\in L_\nu} d^\omega_{z\alpha lt}\, Z^\omega_{z\alpha lt} \le \eta_{z\alpha}\, \beta^\omega_{z\alpha t}\, x^\omega_{z\alpha t},\ z\alpha \in R,\ \bigcup_\nu L_\nu = L,$$

$$\sum_{l\in L_\nu} d^{\kappa\omega}_{s\alpha lt}\, y^{\kappa\omega}_{s\alpha lt} \le \eta_{s\alpha}\, \beta^\omega_{s\alpha t}\, q^\omega_{s\alpha t},\ s\alpha \in S,\ \bigcup_\nu L_\nu = L, \tag{23}$$

$$Z^\omega_{z\alpha lt} \ge \eta_{z\alpha}\, \underline{Z}^\omega_{z\alpha lt},\ y^{\kappa\omega}_{s\alpha lt} \ge \eta_{s\alpha}\, \underline{y}^{\kappa\omega}_{s\alpha lt},\ z_\alpha \in R,\ s\alpha \in S,$$

by constraints of non-equality type, caused by insufficiency of "non-water" resources and production targets of water-consuming industries:

$$\sum_{z\alpha\in R} m^d_{z\alpha}\, \eta_{z\alpha} \le M^d,\ d \in D_I,$$

$$\sum_{t\in[To,\ T]} [\sum_{z\alpha\in R} \varphi^{d\omega}_{z\alpha t}(x^\omega_{z\alpha t}, u^{d\omega}_{z\alpha t}) + \sum_{s\alpha\in S_{II}} \varphi^{\kappa d\omega}_{s\alpha t}(x^{\kappa\omega}_{s\alpha t}, u^{\kappa d\omega}_{s\alpha t})] \le M^{d\omega},\ d \in D_{II}, \tag{24}$$

$$\sum_{z\alpha\in R} \varphi^{d\omega}_{z\alpha t}(x^\omega_{z\alpha t}, u^{d\omega}_{z\alpha t}) + \sum_{s\alpha\in S_{II}} \varphi^{\kappa d\omega}_{s\alpha t}(x^{\kappa\omega}_{s\alpha t}, u^{\kappa d\omega}_{s\alpha t}) \le$$

$$M^{d\omega}_t,\ d \in D_{III}$$

by conditions of interaction between characteristic functions of WRS elements' development alternatives and rules of formation of pollutants' complexes:

$$\eta_{z\alpha} \in |0;1|,\ \sum_{z\alpha\in a_z} \eta_{z\alpha} = 1,\ z \in R, \tag{25}$$

$$u^{d\omega}_{z\alpha t} = \sum_{l\in L} \delta^{dl\omega}_{z\alpha t}\, y^\omega_{z\alpha lt},\ u^{\kappa d\omega}_{s\alpha t} =$$

$$\sum_{l\in L} \delta^{\kappa dl\omega}_{s\alpha t}\, y^{\kappa\omega}_{s\alpha lt},\ z\alpha \in R,\ s\alpha \in S_{II} \tag{26}$$

and, finally, by initial conditions:

$$q^\omega_{s\alpha t} = q^{\omega\circ}_{s\alpha t},\ y^\omega_{s\alpha lt} =$$

$$y^{\omega\circ}_{s\alpha lt},\ s_\alpha \in S,\ t \in [To - \theta^\omega_{s\alpha t},\ To - 1], \tag{27}$$

$$Q_{i\alpha o} = Q^\omega_{i\alpha o} = Q^\omega_{i\alpha T} = Q_{i\alpha T},\ Y_{i\alpha o} = Y^\omega_{i\alpha o} = Y^\omega_{i\alpha T} = Y_{i\alpha T},\ i\alpha \in I.$$

In the task A the system of equations (19) is received from (12) by the substitution of interconnection equations (2) of inlet and outlet arc flows and equations (5) for the relationships of water losses from reservoirs and seas; coefficient of "storage gain" $K^\omega_{i\alpha t} = 1 - h_t\, \gamma^\omega_{i\alpha t}$. The system of equations (20) is received by the substitution of equations (9) of pollutant storage supplies in the network $\Gamma(J, S)$ into (13).

Task A is a two-staged task of stochastic programming, in which first-stage strategic variables are characteristic functions of development alternatives of the system η, second-stage tactical variables are vectors of water and pollutant supplies Q and Y in storages and water flows q and pollutant flows y in the arcs of $\Gamma(J, S)$.

8 SOLUTION OF THE PROBLEM

Task A is multiextremal, i.e. it has local minima, different from the global one. Multiextremity of

this task is caused by the non-convexity of the biseparable task function (18) and non-convexity of the permissible set G, assigned by bilinear constraints of the equation (22), biseparable non-convex constraints of the equation (24) and integer requirements (25) of strategic variables η. Specific features of the task A allow us to find methods of its solution.

This solution is reduced to the selection of optimum vectors of a finite sequence of estimating convex tasks on the graph $\Gamma(J, S)$. working out details of the diagram of branches and boundaries, (Lazebnik et al. 1981). As a result, the vector is obtained, corresponding to the value of the task function, different from the optimum one by not more than the prescribed value and exceeding the permissible set by not more than the prescribed error. This method is described in detail elsewhere, (Lazebnik et al. 1981).

REFERENCES

Instructions on calculation method of mixing and dilution of sewage in rivers, lakes and water storage basins. 1971. Transections of VODGEO, 224 p., (in Russian).

Lazebnik, A.I., Khranovich, I.O., & Tsallagova, O.N. 1981. General separable tasks and their application. Avtomatika i Telemekhanika 8: 107—118, (in Russian).

Priazhinskaya, V.G & Khranovich, I.L. 1978. Water resources system optimum control. — In: Urban Regional and National Water Planning, Proc. IFAC Workshop, Kyoto, 1977, Oxford: 139—146.

Vavilin, V.A. & Tsytkin, M.U. 1977. Mathematicall modelling and water environment quality control. Vodnye Resursy 5: 114—132, (in Russian).

EXPERIMENTAL-ANALYTICAL METHOD OF MODELLING TRANSFORMATION OF NATURAL ORGANIC MATTER IN WATER STORAGE RESERVOIRS

Andrey Kocharian[1], Valentin Gekov[2], Alexander Malyutin[1] & Igor Lapin[2]

KOCHARIAN, A., GEKOV, V., MALYUTIN, A., & LAPIN, I. 1989. Experimental-analytical method of modelling transformation of natural organic matter in water storage reservoirs. Publications of Water and Environment Research Institute, National Board of Waters and the Environment, Finland, No. 3.

The paper presents the method of forecasting non-conservative substances transformation, based on the substitution of particle trajectory analysis by that of the time of their residence in the reservoir. The residence time distribution (RTD) function is the basic characterizing pattern and intensity of water circulation. The value of this function at a given moment of the time is the probability that a flow element, entering the reservoirs at the initial moment, will stay in it during a period shorter, than the said time. The RTD function values for different water bodies were obtained experimentally on the basis of physical models. They allow us to calculate the level of the processes of non-conservative substance transformation. The suggested method was used to study humic organic substances transformation in the Uchinsk reservoir, which is the source of water supply of Moscow. A good agreement between observed and calculated data is obtained.

Index words: function of residence time distribution (RTD function); hydraulic model; hydrodynamic structure of water circulation; non-conservative substance transformation.

[1] Water Problems Institute of the USSR Academy of Sciences, 103064, Moscow, USSR
[2] Hydrochemical Institute of the USSR State Hydrometeorological Committee, 344091, Rostov-na-Dony, USSR.

1 INTRODUCTION

River flow management is important for the composition of the water, which is manifested by different mean values of the river water chemical composition, its redistribution in time, changes in the velocity and duration of transformation processes, involving organic and organic-inorganic allochthonous compounds, as well as intensification of autochthonous matter synthesis. The paper considers basic factors, governing transformation of natural organic matter in water storage reservoirs.

The intensity of water circulation, determing

the duration of the effect, exercised by physical, chemical and biological processes on autochthonous and allochthonous organic matter, is an important factor of substances transformation in reservoirs. Present-day theoretical approaches to describe the reservoir velocity fields, based on combined integration of equations in terms of hydrodynamics and physics-chemical kinetics are rather difficult to apply, since the complicated geometry of boundary conditions characteristic of inflows does not ensure correct solutions (Kafarov 1985).

2 DESCRIPTION OF THE MODEL

The method, developed at the Water Problems Institute of the USSR Academy of Sciences is based on substituting the analysis of particles trajectories by that of their residence time in the reservoir. The RTD function is a key factor in describing the water circulation intensity and pattern. For flowing water reservoirs the RTD function is clear: its value at a given moment is the probability that a flow element entering the reservoir at the initial (zero) time t_o would stay in it during a period, shorter than the said t-time. Substances transformation processes in a given reservoir develop with time and different flow elements reside in the reservoir during different periods of time, which means that the RTD function allows us to assess the level of transformation processes of a given substance.

The RTD function is equivalent to an impulse transient function of the system. In case of water storage reservoirs the impulse transient function is represented by a curve of variation in substance concentration at the outlet, the substance inflow at the inlet being of volley type. In a dynamic system (reservoirs) it is impossible to determine the impulse transient function directly. So the RTD functions are experimentally obtained from hydraulic investigations employing water reservoir models.

Theoretically, the hydraulic modelling is based on the Navier-Stokes and continuity equations. Investigation data attest to a possibility of using forced flows, provided both geometric and dynamic similarity could be achieved. When the data inferred from the model are extended to real-life objects, the indices of inner water circulation intensity in reservoirs are not appreciably affected by the employed forced flows and model distortions (Gordin 1984).

Model experiments allow us to obtain the data on the curves of a hydrodynamic system response to a pulse injection of chemical indicator. Besides, hydraulic experiments provide ground for obtaining an idealized hydrodynamic pattern of water circulation in the given reservoir. The hydrodynamic structure is divided into ultimate blocks and units regarded as simple with respect to the mathematical description of the hydrochemical processes. These units are thoroughly studied hydrodynamic structures of mixer type. Such division results in substituting the actual hydrodynamic structure by an equivalent schematic description, calculated from equations of mass balance. If each of units has a corresponding differential equation, the combination of differential equations for all the units, coupled with algebraic equations of mass balance for nodal points of the block scheme, constitutes a mathematical model of the whole reservoir. Individual schemes of water circulation also require individual structure of mathematical description concerning the reservoir dynamic characteristics, that is RTD function. With multi-unit ramified schemes of water circulation the reservoir dynamic characteristic result in rather sophisticated models. Bearing it in mind, it is reasonable to substitute the individual water circulation scheme by a dynamically equivalent typical structure of longitudinal-transversal water circulation with the parameters with the providing the required RTD function at the reservoir outlet. The parameters of this model are computer-selected following the criterion of minimum deviation of the model RTD functions from the experimental ones, (Gordin 1984, 1987; Gordin and Kocharian, 1978).

This idea can be illustrated by the data obtained from studying water circulation processes and organic matter transformation at the Uchinsk reservoir with volume 0.146 km^3, utilized for water supply of Moscow. This reservoir was simulated after the Froude criterion, scale relation being:

$$\alpha_v = \frac{\alpha_n}{\alpha_e^{0.5} \cdot m}; \alpha_g = \frac{\alpha_e^{0.5} \cdot \alpha_h^2}{m}; \alpha_t = \frac{\alpha_e^{1.5} \cdot m}{\alpha_n} \quad (1)$$

where α_v, α_g, α_t, α_e and α_n are scale coefficients of velocity, flow, time, vertical and linear dimensions respectively; m is the degree of flow forcing in the model. The model was run with a nine-fold distortion of scale ($\alpha_e = 900$, $\alpha_n = 100$).

Curves of reservoir response to an indicator injections with a stable chemical component were inferred from the results of ten fluorescein injections with a stationary functioning of the

model. Scattering of the experimental RTD functions proved to be insignificant and the obtained data could be averaged, (Fig. 1a). Model experiments allowed us to identify the main flow patterns, (Fig. 2a). The experiments provided a sound basis for compiling a block-scheme of water circulation, (Fig. 2b), substituted with a dynamically equivalent unified one with the parameters providing the same value of the RTD function, (Fig. 1b). Parametrical identification of the reservoir mathematical model employs this unified structure of longitudinal-transversal water circulation. Each cell represents a mixer. The model parameters of each tract are as follows: net lag time τ, number of unified two-cell n blocks, time constant of a unified block T, relative volume of slow water zone x, relative intensity of water circulation between the transit and slow water zones y. These parameters were computer-selected through relative search following the criterion of maximum approximation of computer model response to δ-functional impact to the experimental RTD function. Deviation of the final solutions from the hydraulic model regressive RTD function does not exceed 10 % in the maximum range and 20 % — in the tails of experimental curves for both tracts. Final parameters of the simulated water exchange in the Uchinsk reservoir are as follows:

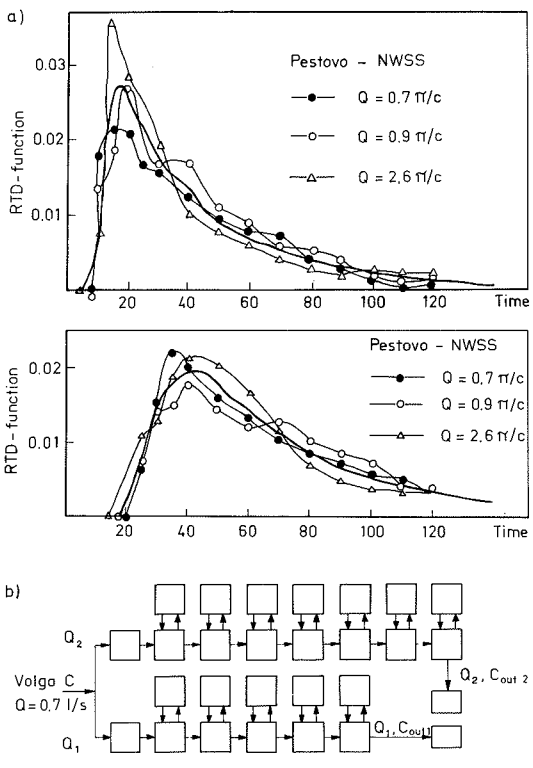

Fig. 1. Experimental RTD function of the hydraulic model, describing the Uchinsk water storage reservoir along the tracts "Pestovo — NWSS" and "Pestovo — EWSS" (a), and the model of water circulation, based the unified structures of longitudinal — transversal water circulation (b).

"Pestovo — Northern Water Supply Station" (NWSS):
$\tau_1 = 4.0$ days, $n_1 = 5$, $T_1 = 7.4$ days, $x_1 = 0.55$, $y_1 = 0.30$;
"Pestovo — Eastern Water Supply Station" (EWSS):
$\tau_2 = 13.1$ days, $n_2 = 7$, $T_2 = 6.9$ days, $x_2 = 0.55$, $y_2 = 0.35$.

It should be noted that net lags of mathematical model are appreciably less than those of response curves; this is assigned to the fact that the mathematical model summed lags which should coincide with the last ones of the response curves, including both the said τ_1 and τ_2 and those emerging in the integration of longitudinal-transversal water circulation equations. With $n = 6$—7 and the total residence time of many days, the last lags are considerable and amount to 2 days for the first tract and 5 days — for the second one. Summed up with τ_1 and τ_2, they amount to 6-day travel time lags at the NWSS and to 18-day lags — at the EWSS.

Retrospective verification and refinement of the water circulation mathematical model was carried out on the basis of field observation data obtained at the reservoir inlet and outlet. Weekly measurements of chloride concentration over the period of 1973—1979 served as statistical data. Chloride content variations reveal a clear seasonal periodicity in conformity with general changes in mineralization due to varied types of water withdrawal throughout the year. This makes it possible to carry out the dynamic investigations for one oscillation frequency $C_{i\,n}$ ($\omega = 0.017$ day^{-1}).

Over the period of 1973—1979 the NWSS and EWSS capacities were relatively stable: $Q_1 = 11.1$ m^{3}s^{-1} and $Q_2 = 15.1$ m^{3}s^{-1}. In accordance with the developed model the reservoir time constants should be as follows: $\tau_1 = 5.4$ days, $T_1 = 10.0$ days, $\tau_2 = 13.0$ days, $T_2 = 6.9$ days.

Now we can calculate amplitude-phase transformation of seasonal variations in the non-conservative admixture concentration, that should be observed over the period if the model is correct. In conformity with the mathematical model

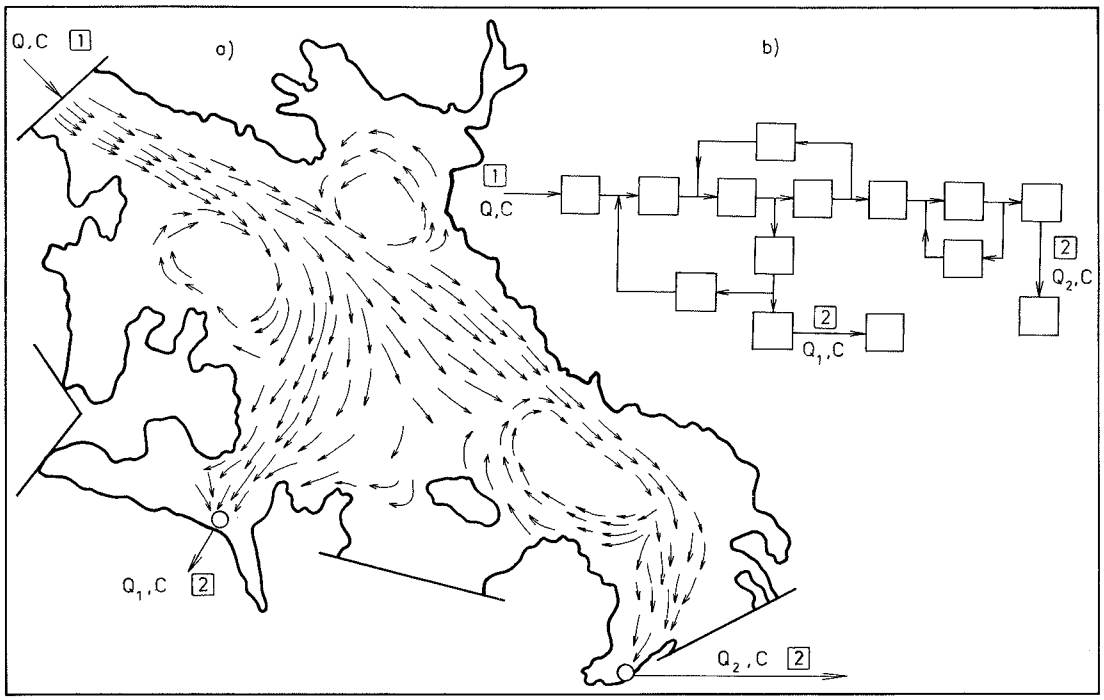

Fig. 2. Scheme of the main currents in the Ucninsk water storage reservoir after experiments with the use of a hydraulic model (a) and the corresponding generalized scheme of water circulation (b).

structure, transformation of cyclic variations in the conservative admixture concentration by each reservoir tract is: (2)

$$A(\omega) = \left| \frac{(\frac{\alpha}{\beta} T\omega)^2 + 1}{[1 - \frac{\alpha(1-\alpha)}{\beta} T^2\omega^2]^2 + [(1 + \frac{\alpha}{\beta}) T \cdot \omega]^2} \right|^{\frac{n}{2}}$$

$$\varphi(\omega) = n[\text{arc tg } \frac{\alpha}{\beta} T\omega - \text{arc tg } \frac{(1 + \frac{\alpha}{\beta}) T \cdot \omega}{1 - \frac{d(1-d)}{\beta} T^2\omega^2}] - \omega\tau \quad (3)$$

3 VERIFICATION OF THE MODEL

Substitution of the parameters n, α, β, τ, and T gives a transformation model $C_{in} - C_{out}$, corresponding to $Q_1 = 11.1$ m^{3}s^{-1}, $Q_2 = 15.1$ m^{3}s^{-1}. Substituting $\omega = 0.017$ day^{-1} into the model we pass on to quantitative evaluation of amplitude suppression and phase shift defining yearly variations in the conservative admixture concentration cited in the first line of Table 1. The second line gives amplitude suppression and phase shift values of yearly variations in chloride content from field investigation data with the first harmony of expansion into a Fourier series of autocorrelation function $R_{C_{in}}$ (Q) and the intercorrelation function $R_{C_{out}}$ (Q).

Table 1. Retrospective verification of the water circulation mathematical model for smoothing down the year cycle of chloride concentration.

	Pestovo-NWSS		Pestovo-EWSS	
	amplitude suppression	phase shift	amplitude suppression	phase shift
Reservoir mathematical model ($Q_1 = 11.1$, $Q_2 = 15.1$)	0.825	50.8	0.881	58.7
Field observation data 1973—1979	0.847	45.2	0.814	52.7

The comparison of actual amplitude-phase transformation with those calculated by the model suggests that the water circulation model, based on the data obtained from experiments, proved to be valid. In order to fit fully the field observation data, the model has been refined following the solution of error equations for A and φ. The final version of water circulation model for the Uchinsk reservoir is $\tau_1 = 53/Q_1$, $T_1 = 99/Q_1$, $n_1 = 5$, $\alpha_1 = 0.55$, $\beta_1 = 0.27$; $\tau_2 = 190/Q$, $T_2 = 101/Q$, $n_2 = 7$, $\alpha_2 = 0.55$, $\beta_2 = 0.14$.

4 THE MODEL APPLICATION

The model can be used to calculate water circulation and the degree of conservative matter averaged in the reservoir with any capacities of EWSS and NWSS, ranging from 10 to 20 m^3/day. Models of this type are basic ones for simulating transformation processes, involving non-conservative admixtures.

One of the main water quality indicators is color. It determined the pattern of water treatment at NWSS and EWSS. It is common knowledge, that the main contribution to the natural water color is made by humic substances (HS), composed of mixed humic acids (HA) and fulvic acids (FA). From the available data of long-term observations of water color at the Ivankovo reservoir, as well as HA and FA content, we have formulated empirical relationship color vs HA concentration for the given reservoir on function of different hydraulic phases:

$$C_{HA} = 0.0563\ e^{0.0174\ A} \quad \text{for the summer-autumn period,} \tag{4}$$

$$C_{HA} = 0.0004\ A^{1.533} \quad \text{for the winter-spring period,} \tag{5}$$

where C_{HA} is the concentration of HA in mg Cl^{-1}, A is the color index in degrees of Platinum-Cobalt scale.

To complete the data on the content and composition of the dissolved organic matter, the FA concentration can be inferred from the C_{HA}/C_{FA} ratio, defined over different periods of time and equal to 0.4 in summer-autumn and to 0.12 in winter-spring. For the water circulation conditions, described by the model and the mathematically postulated concentrations of color index at the inlet mC_{in} and outlet mC_{out}, we have:

$$\frac{m\,C_{out}}{m\,C_{in}} = \frac{(\frac{\alpha}{\sqrt{\beta}}\,T \cdot K + 1)^n \cdot e^{-\kappa\tau}}{[\frac{\alpha(1-\alpha)}{\beta}\,T^2K^2 + (1 + \frac{\alpha}{\beta})\,T \cdot K + 1]^n} \tag{6}$$

where K is a seasonal constant of the reservoir auto-purification capacity, expressed in $days^{-1}$.

According to the statistics of observations, in 1973—1979 we had:

$$\eta_1 = mC_{out}/mC_{in} = 45.2°/54.2° = 0.834;$$
$$\eta_2 = mC_{out}/mC_{in} = 43.3°/54.2° = 0.799.$$

Therefore, in order to determine the average annual K value, it is sufficient to substitute hydrodynamic parameters τ, n, T, α, β and η of the corresponding tract and solve the obtained transcendent equations by famous numerical methods. As a result we obtain the same K value for both the tracts, (with the accuracy up to the fourth digit): $K = 0.0039\ day^{-1}$. For the winter period $K = 0.0019\ day^{-1}$.

A better understanding of autopurification processes made further investigations necessary. They concerned the processes of elimination of naturally dissolved organic substances (HA and FA) in water bodies. The experiments improved our knowledge of HA and FA sedimentation, caused by changes of the reservoir hydrochemical conditions. The results, yielded by the study of HA phase dispersion composition under various environmental conditions, using the exclusion and ion-exchange chromatography, ultrafiltration and ultra-violet spectroscopy, suggest the following sedimentation of HA depend on the quantitative and qualitative composition of inorganic components and proceeds in a step-wise manner. On the whole, HA sedimentation is a combination of successive competitive processes. Cations of alkali-earth metals interact with low-molecular fractions (LMF) of the HA and partially neutralize the surface charge of macromolecules. Reduction of the repulsive force between macromolecules leads to the formation of larger aggregates, i.e. high-molecular fractions (HMF). Later on a similar interaction of Ca^{2+} cations and HMF results in enlarged Ha aggregates up to the size of colloid fraction (CF) and further to suspended fraction (SF), which means the formation of solid phase (SP).

A mathematical model of HA sedimentation has been developed on the basis of the described mechanism, The model includes a system of ordinary differential equations of the first order:

$$d[S_1]/d\tau = \beta_1 [LMF] \cdot [S] \quad (7)$$

$$d[S_2]/d\tau = \beta_2 [HMF] \cdot [S] \quad (8)$$

$$d[S_3]/d\tau = \beta_3 [CF] \cdot [S] \quad (9)$$

where S is the resultant concentration of inorganic components; S_1, S_2, S_3 are the concentrations of inorganic components in each of the described processes; τ is the time.

Current concentrations of the HA fractions in the interaction process are inferred from:

$$[LMF] = [LMF_o] - 0.2 [S_1] \quad (10)$$

$$[HMF] = [HMF_o] - 0.5 [S_1] - 0.05 [S_2] \quad (11)$$

$$[CF] = 0.01 [S_2] - 1.10^{-4} [S_3] \quad (12)$$

$$[S] = [S_o] - [S_1] - [S_2] - [S_3] \quad (13)$$

Initial LMF and HMF concentrations are given with index "0".

5 CONCLUSION

The suggested method ensures a considerable simplification of mathematical models, describing non-stationary processes of natural organic substances transformation in water storage reservoirs. This method was successfully verified and practically tested in the process of investigating chemical-technological processes. This method can be used in forecasting water quality in reservoirs —this was shown at the example of thoroughly investigated Uchinsk reservoir. A good agreement between observed and calculated values allows us to recommend the use of this method in planning the development of water supply stations.

The model, describing sedimentation of various organic fractions of humic nature ensures the identification of the main trends in the process of different HA forms' occurrence, helps us to recognize types of interconnection between them and determine relative kinetic parameters, characterizing these processes, and thus take into account, quantitatively assess the rate of HA sedimentation in natural water bodies.

ACKNOWLEDGEMENTS

We wish to thank the Head of the Chemical Laboratory of the Akulovo Hydraulic Structure Doctor Yu.S.Datsenko for his help in carrying out experiments and for the materials on the chemical composition of the Uchinsk reservoir water.

REFERENCES

Gordin, I.V. 1984. Modelling and computer identification of the process of longitudinal-transversal pollutant transport in water bodies and streams. Transactions of VODGEO, p. 15—23, (in Russian).

Gordin, I.V. 1987. Technological systems of water treatment. Moscow, 264 p., (in Russian).

Gordin, I.V. & Kocharian, AS.G. 1978. The RTD function of water masses in reservoirs. Vodnye Resursy 1: 103—114, (in Russian).

Kafarov, V.V. 1985. Methods of cybernetics in chemistry and chemical technology. Moscow, 448 p., (in Russian).

Znamenskiy, V.A. 1984. Hydrological processes and their role in water quality formation. Leningrad, 248 p., (in Russian).

LIST OF SYMBOLS

A = color index deg. of Pt—Co
CF = colloid fraction of humic acids
C_{FA} = fulvic acids concentration
C_{HA} = humic acids concentration
C_{HS} = humic acids concentration
EWSS = Pestovo-Eastern Water Supply Station
HMF = high-molecular fractions of humic acids
K = seasonal constant of the reservoir auto-purfication capasity
LMF = low-molecular fractions of humic acids
NWSS = Pestovo-Northern Water Supply Station
n = number of unified two-cell blocks
m = degree of flow routing in hydraulic model
RTD = residence time distribution
S = resultant concentration of inorganic processes
SF = suspended fraction of humic acids

SP = solid phase
S_1, S_2, S_3 = concentrations of inorganic components in various processes
T = time constant of a unified block
x = relative volume of slow water zone
y = relative intensity of water circulation between the transit and slow water zones
α = parameter in amplitude-phase transformation
α_g = flow scale coefficient of the hydraulic model
α_l = vertical scale coefficient of the hydraulic model
α_n = linear scale coefficient of the hydraulic model
α_t = time scale coefficient of the hydraulic model
α_v = velocity scale coefficient of the hydraulic model
β = parameter in amplitude-phase transformation
ω = oscillation frequency
τ = net lag time

SEAWATER INTRUSION INTO ESTUARIES AND AQUIFERS

Martin G. Khublaryan[1)]
Anatolii P. Frolov[1)]

KHUBLARYAN, M.G. and FROLOV, A.P. 1989. Seawater intrusion into estuaries and aquifers. Publications of water and Enviroment Research Institute, National Board of Waters and the Enviroment, Finland. No. 3.

Study of sea-water intrusion into estuaries, mouth areas of rivers, and aquifers has become recently and urgent scientific and applied problem due to the high-rate withdrawal of fresh water from rivers and aquifers in coastal areas. The paper formulates mathematical models and gives some approximate analytical solutions of problems of saline-water intrusion into estuaries and fresh-water aquifers. Unsteady one-dimensional models of convective salt transfer in an estuary with a variable cross-section and steady circulating flows in a two-dimensional, vertically slightly stratified river mouth have been examined. The problem of defining the interface between fresh and saline waters in a confined aquifer has been also discussed both for movement of two immiscible liquids and with consideration of salt convective diffusion.

Index words: estuary, aquifer, seawater intrusion, simulation.

[1)] Water Problems Institute of USSR Academy of Sciences, 103064 Moscow, USSR.

1 SEAWATER INTRUSION INTO ESTUARIES

The mixing of fresh river and salt sea waters in estuaries and river mouths has become a major subject of oceanological, hydrological, and ecologo-economic research because the intensive water intake from river drainage areas disturbs the natural equilibrium of water masses near the coasts.

1.1 Well-mixed estuaries

In well-mixed estuaries, water salinity does not practically vary depth wise; fresh water moves seawards and sea water landwards by horizontal turbulent diffusion. At any depth the overall water flux is sea-bound.

Salt transfer in a well-mixed valley-type estuary is often described by one-dimensional mathematical models of convective diffusion which may

be obtained by integrating three-dimensional unsteady-state equation describing turbulent diffusion of solutes along the variable cross-section of the estuary. The one-dimensional equation of convective diffusion takes the form

$$\frac{\partial c}{\partial t} + v\frac{\partial c}{\partial S} = D\frac{\partial^2 c}{\partial S^2} + \frac{F'(S)}{F(S)} D\frac{\partial c}{\partial S} + q(S), \qquad (1.1)$$

where c is the solute concentration; t is the longitudinal (axial) coordinate; v is the fluid velocity; D is the constant factor of turbulent diffusion; q is the intensity of solute sources along the path; and F(s) is the cross-sectional area of the estuary.

If the cross-sectional area varies exponentially

$$F(S) = F_o\,(S/S_o)^n \qquad (1.2)$$

equation (1.1) can be rearranged into

$$\frac{\partial c}{\partial t} + v\frac{\partial c}{\partial S} = D\frac{\partial^2 c}{\partial S^2} + \frac{nD}{S}\frac{\partial c}{\partial S} + q \qquad (1.3)$$

where F_o is the cross-sectional area with $S = S_o$.

An equation similar to (1.3) has been used by Karaushev and Meerovich (1981) to simulate the zone of pollution by nonconservative matter with a negligible advective transfer. In estuaries where the inflow of fresh water is noticeable, this transfer cannot be ignored, otherwise large errors may occur.

Let us take up several examples of solving equation (1.3) analytically. When there are no sources in a channel whose cross-sectional area is constant (n = 0), we have from equation (1.3)

$$\frac{\partial c}{\partial t} + v\frac{\partial c}{\partial S} = D\frac{\partial^2 c}{\partial S^2} \qquad (1.4)$$

By introducing dimensionless parameters η and τ

$$S = \eta L,\ t = L^2\tau/D \qquad (1.5)$$

where L is the characteristic linear scale, equation (1.4) is rearranged into

$$\frac{\partial c}{\partial \tau} + \beta\frac{\partial c}{\partial \eta} = \frac{\partial^2 c}{\partial \eta^2},\ \beta = \frac{vL}{D} \qquad (1.6)$$

With boundary conditions

$$\tau = 0,\ C = 1;\ \eta = 0,\ c = 1;\ \eta = \infty,\ c = 0 \qquad (1.7)$$

equation (1.6) is

$$c(\eta, \tau) = \frac{1}{2}\left[\operatorname{erfc}\left(\frac{\eta - \beta\tau}{2\sqrt{\tau}}\right) + e^{\eta\beta}\operatorname{erfc}\left(\frac{\eta + \beta\tau}{2\sqrt{\tau}}\right)\right] (1.8)$$

where $\operatorname{erfcu} = 1 - \frac{2}{\sqrt{\pi}}\int_o^u e^{-\xi^2}\,d\xi$

Let us use equation (1.4) to simulate the convective-diffusional transfer of fresh river water in a mass of sea water with allowance for evaporation. Introducing the dimensionless variables η and τ of equation (1.5), the boundary-value problem

$$\frac{\partial c}{\partial \tau} + \beta\frac{\partial c}{\partial \eta} = \frac{\partial^2 c}{\partial \eta^2} - \alpha,\quad \alpha = \frac{qL^2}{D}, \qquad (1.9)$$

$$\tau = 0,\ c = 0;\ \eta = 0,\ c = 1;\ \eta = 1,\ c = 0$$

is solved as a trigonometric series

$$c = \bar{c} + \sum_{K=1}^{\infty} B_{1K}\exp\left(\frac{\beta\eta}{2} - \lambda_K^2\tau\right)\operatorname{Sin} K\pi\eta, \qquad (1.10)$$

where

$$\lambda_K^2 = K^2\pi^2 + \frac{\beta^2}{4},$$

$$C = 1 - \frac{\alpha\eta}{\beta} - \frac{(1 - \frac{\alpha}{\beta})(1 - \exp\beta\eta)}{1 - \exp\beta},$$

$$B_{1K} = \frac{8\pi K}{4\pi^2K^2 + \beta^2}\left[\frac{\alpha}{\beta}\left|(-1)^{K+1}\pi\exp\left(-\frac{\beta}{2}\right) =\right.\right.$$

$$= \frac{4\pi\beta}{4\pi^2K^2 + \beta^2}\left(1 + (-1)^{K+1}\exp\left(-\frac{\beta}{2}\right)\right)\Big| +$$

$$+ \left(\frac{1 - \frac{\alpha}{\beta}}{1 - \exp\beta} - 1\right)\Big|1 + (-1)^{K+1}\exp\left(-\frac{\beta}{2}\right)\Big| -$$

$$\left. - \frac{1 - \frac{\alpha}{\beta}}{1 - \exp\beta}\Big|1 + (-1)^{K+1}\exp\left(\frac{\beta}{2}\right)\Big|\right]$$

and q is the constant evaporation rate minus precipitation (q > 0). If on the left-hand side $\eta = 0$, the boundary condition of the third kind is specified

$$\frac{\partial c}{\partial \eta} + \beta(1 - c) = 0 \qquad (1.11)$$

then we have instead of (1.10)

$$c = \bar{c}_1 + \sum_{K=1}^{\infty} B_{2K} \exp\left(-\frac{\beta\xi}{2} - \lambda_K^2 \tau\right) \operatorname{Sin} \eta_K \xi, \tag{1.12}$$

where

$$\xi = 1 - \eta,\ \bar{c}_1 = \frac{\alpha}{\beta}\xi + \left(1 - \frac{\alpha}{\beta} - \frac{\alpha}{\beta^2}\right),\ \lambda_K^2 = \eta_K^2 + \frac{\beta^2}{4},$$

$$\tan \eta_K + \frac{2\mu_K}{\beta} = 0,$$

$$B_{2K} = \frac{4\mu_K (a_K + B_K + d_K)}{(2\mu_K - \operatorname{Sin} 2\mu_K)(\beta^2 + 4\mu_K^2)},$$

$$a_K = \frac{2\alpha}{\beta}\left[\beta \exp\frac{\beta}{2} \operatorname{Sin} \mu_K - 2\mu_K \exp\frac{\beta}{2} \operatorname{Cos} \mu_K\right],$$

$$B_K = \frac{4\alpha}{\beta}\left[(\beta^2 + 4\mu_K^2) \exp\frac{\beta}{2} \operatorname{Sin} \mu_K + \right.$$

$$\left. + 4\beta\mu_K \left(1 - \exp\frac{\beta}{2} \operatorname{Cos} \mu_K\right)\right],$$

$$d_K = 2\left(1 - \frac{\alpha}{\beta} - \frac{\alpha}{\beta^2}\right)(2\mu_K \operatorname{Cos} \mu_K - \beta \operatorname{Sin} \mu_K) \exp\frac{\beta}{2}.$$

For an expanding estuary of constant depth H, we have from equation (1.3) with n = 1

$$\frac{\partial c}{\partial t} = D\frac{\partial^2 c}{\partial \sigma^2} + \frac{\beta_1}{\sigma}\frac{\partial c}{\partial \sigma} - q,\ \beta_1 = D - \frac{Q}{\varphi_e H} \tag{1.13}$$

where σ is the instantaneous radius, φ_e is the estuary expansion angle, and Q is the river discharge.

By introducing dimensionless coordinates as in equation (1.5)

$$\sigma = \zeta L,\ t = \tau L^2/D \tag{1.14}$$

equation (1.13) is rearranged, with q = 0, into

$$\frac{\partial c}{\partial \tau} = \frac{\partial^2 c}{\partial \zeta^2} + \frac{\gamma}{\zeta}\frac{\partial c}{\partial \zeta},\ \gamma = \beta_1/D \tag{1.15}$$

Under the boundary conditions

$$\tau = 0,\ c = 0;\ \zeta = 0,\ c = 1,\ \zeta = \infty,\ c = 0 \tag{1.16}$$

an automodel solution of equation (1.15) can be obtained in the form

$$c(\tau, \zeta) = \Gamma(a, \theta)/\Gamma(a), \tag{1.17}$$

where $\Gamma(a)$ is a gamma-function and $\Gamma(a, \theta)$ is an incomplete gamma-function

$$\theta = \zeta^2/4\tau,\ a = \frac{1-\gamma}{2} > 0.$$

The solution of (1.17) is presented in Fig. 1 with some values of a proportional to the river discharage Q, The area where large amounts of fresh water are present is largely dependent on the parameter a. Thus with c = 0.95 the length of this zone increases 20-fold as a increases from 1 to 4.

For an expanding estuary of finite length with a boundary condition on the right-hand side as

$$\zeta = 1,\ c = 0 \tag{1.18}$$

and other boundary conditions in the form of (1.16), the distribution of the fresh water content c (ζ, τ) can be obtained as a Bessel series of functions

$$c = 1 - \zeta^{2a} + \zeta^a \sum_{K=1}^{\infty} A_K e^{-\lambda_K \tau} I_a(\lambda_K \zeta), \tag{1.19}$$

where λ_K are roots of the equation $Ia(\lambda_K) = 0$,

$$A_K = -\frac{\lambda_K^{a-2}}{I_{a-1}^2(\lambda_K)\, 2^{a-2}\Gamma(a)}$$

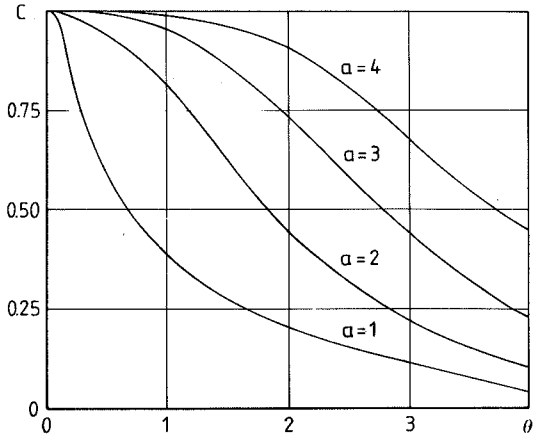

Fig. 1. The effect of river flow on the dynamics of sea water desalination by fresh water in an expanding estuary.

1.2 Partially mixed estuaries

In slightly stratified estuaries, salinity is different in the surface stratum and in deeper waters, with a noticeable transfer through medium depths. The horizontal and vertical salinity gradients exist both in the surface and deeper strata: salt is advectively transferred in surface strata towards the sea and in bottom strata towards the land.

The chief subject of interest in the hydrodynamics of slightly stratified estuaries is the residual circulation in small, relatively narrow estuaries not affected by tides. The estuary is viewed as small when the tidal wave is shorter than the estuary length, but other short-term perturbations such as wind make an impact on the average circulation and mass transfer. Circulation fluxes in estuaries may be classified into lateral and vertical which both result from the action of the same external and internal forces such as wind, tides, topography, river flow and sea water salinity.

For narrow estuaries whose length is assumed to be much larger than the width, the properties of lateral fluid and salt fluxes do not change much. Therefore three-dimensional equations of the estuary hydrophysics can be integrated over the width and reduced to a simpler two-dimensional form. For an estuary, two-dimensional in the vertical plane, slightly stratified, and having a constant depth and width, the equations of motion, continuity, and diffusion of a conservative solute averaged over the tide period for a steady-state case take the form

$$u\frac{\partial u}{\partial x}+v\frac{\partial u}{\partial y}=-\frac{1}{\rho_o}\frac{\partial p}{\partial x}+\frac{\partial}{\partial y}(Axy\frac{\partial u}{\partial y}), \qquad (1.20)$$

$$0=-\frac{1}{\rho}\frac{\partial p}{\partial y}+g,$$

$$0=\frac{\partial u}{\partial x}+\frac{\partial v}{\partial y},$$

$$u\frac{\partial c}{\partial x}+v\frac{\partial c}{\partial y}=\frac{\partial}{\partial x}(Kx\frac{\partial c}{\partial x})+\frac{\partial}{\partial y}(Ky\frac{\partial c}{\partial y})$$

where u and v are the liquid velocity components along the x and y axes, respectively; p and ρ are the liquid pressure and density; A_{xy} is the coefficient of turbulent viscosity; K_x and K_y are coefficients of turbulent diffusion; ρ_o is the density of fresh water, c is the salt content; and g is gravity.

The liquid state equation has the form

$$\rho=\rho_o(1+0.76c) \qquad (1.21)$$

Introducing a function such as ψ (x,y) by the relations

$$u=\frac{\partial\psi}{\partial y},\ v=-\frac{\partial\psi}{\partial x} \qquad (1.22)$$

we have boundary conditions

$$y=0,\ \psi=0,\ \frac{\partial^2\psi}{\partial y^2}=\frac{T}{\rho_o Axy},\ \frac{\partial c}{\partial y}=0, \qquad (1.23)$$

$$y=H,\ \psi=Q,\ \frac{\partial\psi}{\partial y}=0,\ \frac{\partial c}{\partial y}=0,$$

$$\lim C=0,\ \lim\frac{\partial\psi}{\partial x}=0,\ x\to-\infty,$$

where T is wind tension.

An approximate solution of equations (1.20) under the boundary conditions (1.23) can be obtained by the Shvets-Targ method (Frolov and Khublaryan 1984). It provides a fairly accurate description of a two-stratum fluid circulation in actual estuaries where the bottom sea water moves upward towards the land whereas the surface flux is sea-bound.

2 SEAWATER INTRUSION INTO COASTAL AQUIFERS

In case of submarine discharge of ground water at the interface of fresh ground water and saline seawater, a transition zone is formed with a highly variable water salinity ranging from that of fresh water to that of seawater. The location and size of this zone are dictated by seawater density, the rate of subaqueous discharge of ground water and other factors. Construction of water intake structures in coastal regions and intensified pumping of ground water can lead to seawater intrusion into freshwater aquifers and can give rise to the pollution of ground water sources that is difficult to eliminate.

2.1 Flow of immiscible liquids

If the movement of two non-mixing liquids in a porous medium occurs in such a way that one

liquid is stagnant, while the other is under steady-state two-dimensional flow conditions, then analytical solution can be obtained using the hodograph method. Although in this case the interface of two liquids is not known in advance, but the boundary condition at the interface is known, the location of the interface becomes known on the hodograph plane.

Let us consider the vertical section of a fresh-water aquifer that is perpendicular to coast where fresh water having a specific weight γ_f moves above stagnant saline liquid having a specific weight γ_s (Fig. 2).

Let us introduce the complex plane $z = x + iy$ and the complex potential of fresh-water flow $w_1 = \varphi + i\psi$, where ψ is function of current, φ is potential of specific discharge of fresh water flow

$$\varphi = K_f\,(y + \frac{p}{\gamma_f}),\ K_f = \frac{K\gamma_f}{\mu_f}, \tag{2.1}$$

where k_f is constant hydraulic conductivity of porous medium with respect to fresh water, μ_f is viscosity of fresh water.

Boundary conditions for complex potential w_1 have the following form: on AF line which is the line of current

$$\psi = 0,\ y = 0, \tag{2.2}$$

on FE line which is also the line of current

$$\psi = Q,\ y = -L, \tag{2.3}$$

where Q is fresh water discharge per unit of aquifer thickness.

AB line is the boundary between percolation zone and water body, therefore, on this line it can be assumed for the case of small angles α that

$$\psi \approx 0,\ y = -x \cdot \tan\alpha\pi \tag{2.4}$$

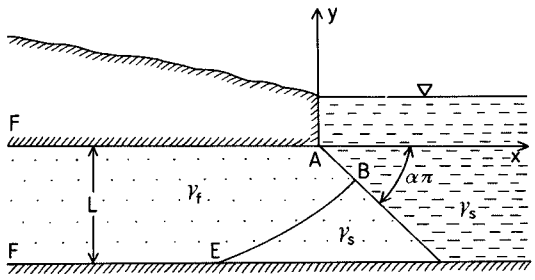

Fig. 2. Schematic diagram of saline water intrusion into a coastal confined fresh-water aquifer through a sloped sea bottom.

The BE line being the line of current simultaneously separates moving fresh water from stagnant saline water. Accordingly, along this line (Polubarinova-Kochina 1977)

$$\psi = Q,\ \varphi = -K'y, \tag{2.5}$$

where $K' = K_f(\gamma_s - \gamma_f)/\gamma_f$

On w_1 plane the semiband AFEB will correspond to AFEB flow area in real physical plane z.

Let us introduce complex velocity of flow

$$w = u + iV, \tag{2.6}$$

where components of liquid flow velocity are determined by the formulas:

$$u = -\frac{\partial\varphi}{\partial x},\ v = -\frac{\partial\varphi}{\partial y} \tag{2.7}$$

Flow areas on w_1 and $w' = \frac{K'}{\bar{w}}$ planes are conformally reflected on auxiliary complex plane ζ (on its upper part).

Using the Kristoffel-Schwartz formula (Polubarinova-Kochina 1977), we obtain the parametric connection of the complex-potential plane with the hodograph plane

$$w'(\zeta) = \frac{1}{\pi}\int_1^{\zeta}\left(\frac{\zeta+1}{\zeta-1}\right)^{\alpha}\frac{d\zeta}{\sqrt{\zeta^2-1}}, \tag{2.8}$$

$$w_1(\zeta) = -\frac{Q\sqrt{B^2-1}}{\pi}\int_1^{\zeta}\frac{d\zeta}{(\zeta-B)\sqrt{\zeta^2-1}} \tag{2.9}$$

Since

$$\frac{dw_1}{dz} = -\bar{w} \tag{2.10}$$

we obtain the conformal depiction of the auxiliary plane ζ on the flow area in the physical plane z:

$$\frac{dz}{d\zeta} = \frac{Q\sqrt{B^2-1}}{\pi K'}\cdot\frac{w'(\zeta)}{(\zeta-B)\sqrt{\zeta^2-1}} \tag{2.11}$$

In order to determine the unknown parameter of conformal reflection B we make use of F points correspondence on the w' plane and on the auxiliary plane ζ

$$\frac{1}{B1} = \frac{\pi K'L}{Q} = \int_1^B \left(\frac{\zeta+1}{\zeta-1}\right)^{\alpha} \frac{d\zeta}{\sqrt{\zeta^2-1}} \qquad (2.12)$$

By integrating the ratio (2.11) in the range from $\zeta = -1$ to $\zeta = +1$, and introducing dimensionless variables

$$\bar{x} = x/L,\ \bar{y} = y/L,\ \bar{x}_B = x_B/L,\ \bar{y}_B = y_B/L,$$

we find the coordinate of B point on the plane z:

$$\bar{x}_B + i\bar{y}_B = \frac{B1\sqrt{B^2-1}}{\pi} e^{-i\alpha\pi} \int_{-1}^{1} \frac{f(\zeta)d\zeta}{(B-\zeta)\sqrt{1-\zeta^2}} \qquad (2.13)$$

where

$$f(\zeta) = \int_{\zeta}^{1} \left(\frac{1+t}{1-t}\right)^{\alpha} \frac{dt}{\sqrt{1-t^2}}$$

The equation for determining the B parameter (2.12) is transformed into

$$\frac{1}{B1} = \int_1^B \left(\frac{\zeta+1}{\zeta-1}\right)^{\alpha} \frac{d\zeta}{\sqrt{\zeta^2-1}} \qquad (2.14)$$

whereas equations of the interface line — into:

$$\bar{y} = \bar{y}_B - B1 \ln\left[\frac{Bp+1}{p+B} + \left(\left(\frac{Bp+1}{p+B}\right)^2 - 1\right)^{\frac{1}{2}}\right], \qquad (2.15)$$

$$\bar{x} = \bar{x}_B - B1\sqrt{B^2-1} \int_B^{chp} \left[\tan\alpha\pi + \int_0^u \left(\frac{chx-1}{chx+1}\right)^{\alpha} dx\right] \frac{du}{chu+B}$$

In Fig. 3 some results of calculations are presented concerning the shape of the stagnant saline wedge using obtained formulas.

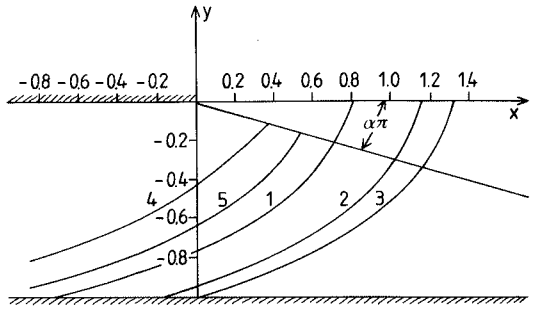

Fig. 3. Dependence of the shape of the fresh and saline water interface on pressure head B1 and sea bottom gradient: 1—3: $\alpha = 0$; 4—5: $\alpha = 0.09$. 1. B1 = 1.0; 3. B1 = 1.5; 4. B1 = 0.2; 5. B1 = 0.3.

2.2 Miscible liquids flow regime conditions

Fresh and saline waters are mixing liquids, and a more or less extended dispersion zone generally lies between them; the size of this zone, dictated by hydrogeological contitions, ranges from several meters to hundreds of meters. The variation of water salinity in the transitional dispersion zone, especially when it is of a comparatively large extent, should be taken into consideration in designing water-intake structures in the zone of coastal aquifers (Goldberg 1976).

Let us consider the section of a confined aquifer, two-dimensional in vertical plane and perpendicular to the coast. Basic equations of the process of saline water intrusion into such an aquifer are: Darcy's law, a continuity equation for liquid, equation of dissolved salt transfer, and equation of liquid state.

Selecting x and y axes of the coordinate system (Fig. 2) in the direction of main axes of anisotropy and bearing in mind that $\delta = (\gamma_s - \gamma_f)/\gamma_f << 1$, we have equations of seepage and continuity for steady-state flow:

$$u = -\frac{Kx}{\mu}\frac{\partial p}{\partial x},$$

$$w = -\frac{Ky}{\mu}\left(\frac{\partial p}{\partial y} + \rho g\right), \qquad (2.16)$$

$$\frac{\partial u}{\partial x} + \frac{\partial w}{\partial y} = 0,$$

where u and w are seepage velocities towards x and y axes, respectively, γ_s and γ_f are specific gravities of saline and fresh water. Introducing ψ current function by the ratio

$$u = \frac{\partial \psi}{\partial y},\ w = -\frac{\partial \psi}{\partial x} \qquad (2.17)$$

and assuming permeability and dispersion coefficients to be constant, we transform equation system (2.16) and diffusion equation to the following form

$$\frac{\partial^2\psi}{\partial y^2}+\frac{Kx}{Ky}\frac{\partial^2\psi}{\partial x^2}=-\frac{\delta Kx\,\gamma_f}{\mu}\frac{\partial c}{\partial x}, \qquad (2.18)$$

$$\frac{\partial\psi}{\partial y}\frac{\partial c}{\partial x}-\frac{\partial\psi}{\partial x}\frac{\partial c}{\partial y}=Dx\frac{\partial^2 c}{\partial x^2}+Dy\frac{\partial^2 c}{\partial y^2}$$

By introducing dimensionless variables

$$\psi=\bar{\psi}Q,\ x=\bar{x}l,\ y=\bar{y}L_z, \qquad (2.19)$$

where L is characteristic length of intrusion zone, L_z is thickness of the aquifer.

Let us substitute (2.19) into (2.18) and equate coefficients at first and third members of the first equation in (2.18) (balance of viscosity and flowability forces). Then we obtain

$$l=L_z Ra/Pe, \qquad (2.20)$$

where

$$Ra=\frac{K_x L_z \delta\gamma_f}{\mu D_y}$$ is Rayleigh number

$Pe=Q/D_y$ is Peclet number.

Omitting the vinculum over variables, we rewrite the system (2.3) in the form

$$\frac{\partial^2\psi}{\partial y^2}+d^2\frac{Kx}{Ky}\frac{\partial^2\psi}{\partial x^2}=-\frac{\partial c}{\partial x},\ d=\frac{Pe}{Ra}, \qquad (2.21)$$

$$\frac{\partial^2 c}{\partial y^2}=dPe\left(\frac{\partial\psi}{\partial y}\frac{\partial c}{\partial x}-\frac{\partial\psi}{\partial x}\frac{\partial c}{\partial y}\right)-d^2\frac{Dx}{Dy}\frac{\partial^2 c}{\partial x^2}$$

According to the data of Lee and Cheng (1974) for aquifers, composed of limestones and coarse-grained sand, the d parameter is equal to 0.04. In this case, in equations (2.21) members with the d^2 coefficient can be ignored, provided $D_x \simeq D_y$, $K_x \simeq K_y$. The system of equations will be presented in a simplified form

$$\frac{\partial^2\psi}{\partial y^2}=-\frac{\partial c}{\partial x}, \qquad (2.22)$$

$$\frac{\partial^2 c}{\partial y^2}=dPe\left(\frac{\partial\psi}{\partial y}\frac{\partial c}{\partial x}-\frac{\partial\psi}{\partial x}\frac{\partial c}{\partial y}\right)$$

with boundary conditions

$$\psi=0,\ \frac{\partial c}{\partial y}=0,\ y=0, \qquad (2.23)$$

$$\psi=1,\ \frac{\partial c}{\partial y}=0,\ y=0$$

$$\lim c=0 \text{ at } x\to-\infty$$

An approximate analytical solution of the above equations was obtained by the authors of this paper in the form of a section of a trigonometric series for c(x,y).

$$c(x,y)=\sum_{K+0}^{n} C_K f_K(x)\,\mathrm{Cos}K\pi y \qquad (2.24)$$

where $f_K(x)=\exp[(1+k)mx]$; m, Ck are unknown constants. Function (2.24) satisfies all the boundary conditions on c(x,y).

Fig. 4 shows the lines of equal salt concentration within the 0.1—0.9 range and stream lines, obtained at different values of n (Frolov and Khublaryan 1980).

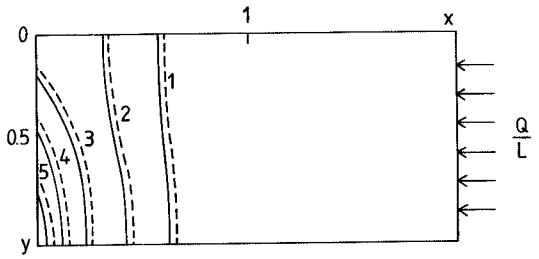

Fig. 4. Distribution of salt concentration in a coastal fresh-water aquifer:
1. c = 0.1; 2. c = 0.3; 3. c = 0.5;
4. c = 0.7; 5. c = 0.9; ——— n = 2; — — — n = 4.

3 CONCLUSION

The developed analytical methods for studying seawater intrusion may be used for estimating water quality variations in estuaries, river mouths, and coastal fresh-water aquifers.

REFERENCES

Frolov, A.P. & Khublaryan, M.G. 1984. Circulation and processes of mixing of river and sea waters in a tideless estuary (in Russian). Vodnye Resursy (Water Resources) 6: 83—88.

Frolov, A.P. & Khublaryan, M.G. 1986. Salt-water intrusion into coastal fresh-water aquifers (In Russian). Vodnye Resursy (Water Resources), 2: 58—63.

Goldberg, V.M. 1976. Hydrogeological forecasts of ground-water quality in water intake areas (In Russian). Moscow, 152 p.

Karaushev, A.V. & Meerovich, L.N. 1981. A model of formation of the stationary zone of water body pollution (In Russian). Meteorologiya i Gidrologia (Meteorology and Hydrology) 1: 105—107.

Lee, C. & Cheng, R.T. 1974. On seawater encroachment in coastal aquifers. Water Resources Research 10(8): 1039—1043.

Polubarinova-Kochina, P.Ya. 1977. Theory of ground water movement (In Russian), Moscow, 664 p.

LIST OF SYMBOLS

A_{xy} = coefficient of turbulent viscosity
B = parameter of conformal reflection
c = solute concentration
D = coefficient of turbulent diffusion
F(s) = cross-sectional area of estuary
g = gravity
H = depth of estuary
K_x, K_y = coefficients of turbulent diffusion
k_f = hydraulic conductivity of porous medium with respect to fresh water
L = characteristic linear scale
L_z = thickness of the aquifer
p = liquid pressure
P_e = Pecklet number
q = intensity of solute sources along the path
Q = river discharge
R_a = Rayleigh number
t = longitudinal coordinate
T = wind tension
u, v = velocity components along x- and y-axes
w_i = complex potential
τ = dimensionless parameter
η = dimensionless parameter
ι = instantaneous radius
φ_e = estuary expansion angle
$\Gamma(a)$ = gamma-function
$\Gamma(a, \theta)$ = incomplete gamma-function
ϱ = density of liquid
ϱ_o = density of fresh water
γ_f = spefic weigth of fresh water
γ_s = spefic weigth of saline water
ψ = function of current
φ = potential of specific discharge of fresh water flow
μ_f = viscosity of fresh water
ζ = auxiliary complex plan

EXAMINATION OF MODEL ADEQUACY AND ANALYSIS OF PHOSPHORUS DYNAMICS IN LAKE KUORTANEENJÄRVI — A CASE STUDY WITH TWO LAKE MODELS

Juhani Kettunen[1], Alexander V. Leonov[2] & Olli Varis[1]

KETTUNEN, J., LEONOV, A.V. & VARIS, O. 1987. Examination of model adequacy and analysis of phosphorus dynamics in Lake Kuortaneenjärvi — A case study with two lake models. Publications of the Water and Environment Research Institute. National Board of Waters and the Environment, Finland. No. 3.

The dynamics of P and algae of Lake Kuortaneenjärvi, Finland, were studied. Two mathematical models were used to analyze the lake behavior. One was tailored for the application with special emphasis on analysis of algal dynamics. The other focuses on P transformations and was transferred with a slight recalibration from Lake Balaton, Hungary and Ivankovskoe Reservoir, USSR. A subtask was to examine and discuss the adequacy of complex ecological lake models in a case of inadequate field data. The results showed that incoming P fractions differed greatly between the two basins of the lake. Organic fractions were more dominating in the lower basin. Net sedimentation was only 20 % of the gross sedimentation. The calibration results of the two models were rather adequate as far as the observed variables were considered but the overparametrization of the models came out in inadequacies of unobserved items. The original scope of the modeling comprised also evidently to the adequacy.

Index words: adequacy, eutrophication, phosphorus, lake model, scope of modeling.

[1] Helsinki University of Technology, Laboratory of Hydrology and Water Resources Management. Rakentajanaukio 4, SF-02150 Espoo, Finland.
[2] Water Problems Institute of USSR Academy of Sciences, 103064 Moscow, USSR.

1 INTRODUCTION

Mathematical models are widely used to study different problems of water quality. Accelerated eutrophication of water bodies due to human activities is a serious environmental problem. It is a subject of comprehensive research using mathematical models. The general purpose of modeling is to assist better understanding of aquatic ecosystems. It also aims in finding reasonable alternatives of system management.

It is inherent that models are simplifications of the real system. They usually consider only a limited amount of problems that are of importance from the point of view of the behaviour of the system. When considering eutrophication usually the topics of interest are the algal and nutrient dynamics. Although these two aspects are closely inter-

related, they may be studied separately by using models of various structures and degrees of complexity. Therefore the results obtained from them should supplement one another to expand our knowledge on eutrophication processes.

The main aim of this work was to study the eutrophication of Lake Kuortaneenjärvi, Western Finland. Two mathematical models were used to analyze the behaviour of the lake. A substask was to examine the adequacy of a complex ecological lake model in the case where only limited amount of field data existed. The work was carried out by using two lake water quality models.

Principally there are several approaches available when constructing an ecological model. One can adopt a model or submodels identified empirically to some other system. Models can be derived from theoretical concepts like "physical laws" or heuristic concepts. In the field of lake modelling two schools having different attitudes towards the choice of the model can be seen. One of the schools emphasizes the lack of general ecological theory and prefers the construction of a model for each case. This sort of argumentation has been presented e.g. by Jørgensen (1983). The other of the schools aims in developing a general lake model, This school originates from the works and philosophy of Park et al. (1974). In this respect, also the two models applied in this study represent different types of approaches. The first of the models rent types of approaches. The first of the models was constructed by decomposing the problem into subprocesses which were independently identified and then coupled together. The second of the models was identified in Lake Balaton, Hungary, then applied to Ivankovskoe Reservoir, USSR (Leonov 1985a) and transferred to Lake Kuortaneenjärvi with a slight recalibration of parameters.

In this paper, the main results gained in this project are concluded and reviewed. The results of eutrophication of Lake Kuortaneenjärvi and the study of adequacy of complex models are referred as case study I and II, respectively.

2 THE DATA AND THE LAKE

The data used was collected from Lake Kuortaneenjärvi in 1980. Altogether 23 sampling instants were carried out for water chemical analyses, temperature and chlorophyll *a*. Algal counts were carried out 10 times. The water budget of the year was constructed according to the daily observations of inflows, outflows and precipitation. The daily records of radiation and wind velocity were obtained from the meteorological stations nearby.

Lake Kuortaneenjärvi (62°45'N, 23°30'E), Finland, suffers from slight eutrophication. The area is relatively densely populated and the recreational use of the lake is abundant. Blooms of blue-green algae embarrass the recreation and fisheries. The main part of nutrient load comes from diffuse sources.

The catchment area is 1280 km^2 half of which is forest and 20 % in agricultural use. The lake has a mean depth of 3.7 m, maximum depth 15 m, mean area 10 km^2 and mean volume $60 \cdot 10^6$ m^3. Water flow is characterized by great fluctuations. Mean outflow was 9 $m^3 s^{-1}$ and the theoretical water residence time ranges from one week during floods in spring and fall to ten weeks in summer. The lake consists essentially of two basins (Fig. 1). Stenmark (1982) gives a detailed description of the lake and the data used in this study.

3 THE MODELS AND THE SIMULATION RESULTS

Two water quality models were calibrated against the field data. One (Varis 1984) was tailored modularly to describer and analyze algal dynamics of Lake Kuortaneenjärvi and the other (Leonov 1985 a, b), identified originally to analyze phosphorus dynamics of Lake Balaton, was transferred and recalibrated slightly for the application.

The Balaton Sector Model (*BALSECT*) is one of the three ecological models developed at the International Institute for Applied Systems Analysis (IIASA) for examining P dynamics and phytoplankton growth within the Lake Balaton eutrophication project. The version used, consisting of seven states and simulating biochemical phosphorus dynamics, is documented by Leonov et al. (1987).

The water quality model for Lake Kuortaneenjärvi, denoted *KUORTANE* in this paper, consists of 15 states. Nitrogen and phosphorus dynamics are considered. The model was originally aimed to describe algal dynamics with a special emphasis on competition facilities of blue-green algae. As an application, a dynamic analysis of impacts of various growth factors is presented by Varis (1986b).

The model input variables consist of 4 and 8

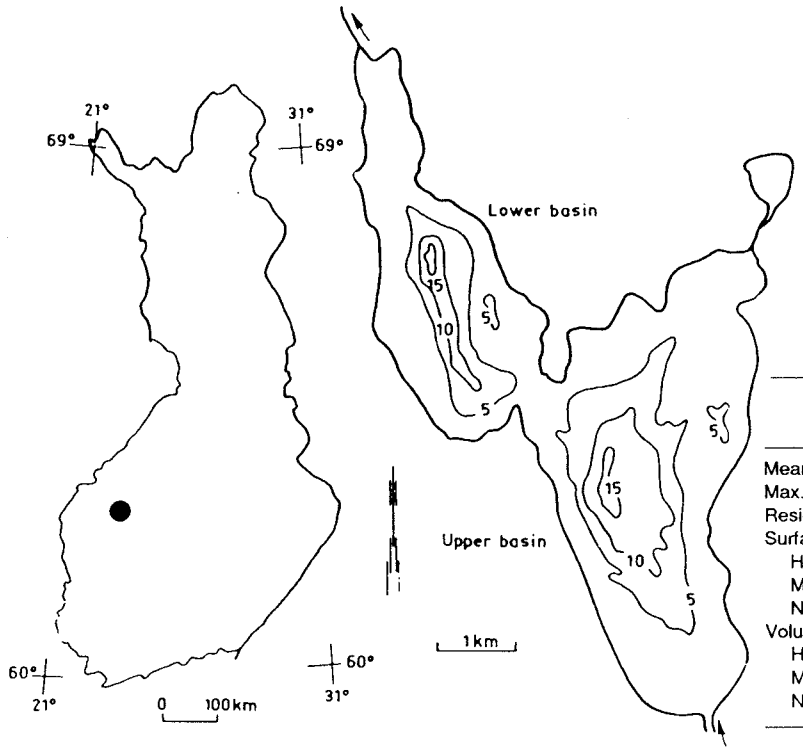

	Whole lake	Upper basin	Lower basin
Mean depth (m)	3.7	4.0	3.2
Max. depth (m)	16	16	16
Residence time (d)	69	49	20
Surface area (km^2)			
HW 1980	18.0	11.9	6.1
MW 1980	16.4	10.9	5.5
NW 1980	15.6	10.5	5.1
Volume (10^6 m^3)			
HW 1980	71.5	50.0	21.5
MW 1980	59.3	42.1	17.2
NW 1980	50.0	36.0	14.0

Fig. 1. Location, bathymetric map and some hydrological characteristics of Lake Kuortaneenjärvi.

external nutrient loads for *KUORTANE* and *BALSECT* respectively. With the application of both models, the lake was subdivided into two continuously stirred basins. The state variables of the models are shown n Table 1 and the flow diagrams in Fig. 2.

As an illustration a part of the calibration results of both models are shown in Fig. 3. Both models appeared to simulate total phosphorus, inorganic particulate phosphate and cholorophyll-*a* concentrations reasonably well. The same holds for the rest of the state variables that have been observed.

4 *CASE I:* PHOSPHORUS TRANSFORMATIONS IN LAKE KUORTANEENJÄRVI

BALSECT — model was used to analyze phosphorus transformations of Lake Kuortaneenjärvi. Detailed desription of the results have been given by Varis et al. (1986) and by Leonov et al. (1987).

For the analysis, the year was discretized into 4 periods (winter, spring, summer and fall). Both of the main basins of the lake were analyzed separately.

According to the simulation results, total phosphorus sedimentation of the lake was about 40 tons during the year. However, due to the mobilization from the sediment, the net sedimentation was only about 8 tons. Most of the total sedimentation took place during the summer period. However, the net sedimentation occurred in spring and fall periods, when the phosphorus load of the lake was about 20 to 40 times the value of summer and winter periods.

The simulation results indicated further that incoming phosphorus fractions differed greatly the two lake basins. The phosphorus loading from river Lapuanjoki into Southern basin was mainly inorganic fractions of phosphorus while the loading from Southern basin into Northern one was to a greater extent autochtonic.

The intensity of biological processes in the Southern basin was higher than in the Northern basin. This was explained by smaller inorganic load to the Northern basin, lower load from the sediment and a shorter retention time.

Table 1. State variables of the models.

BALSECT		*KUORTANE*	
DIP	Dissolved inorganic phosphorus	*DIP*	Dissolved inorganic phosphorus
DOP	Dissolved organic phosphorus	*DIN*	Dissolved inorganic nitrogen
PD	Unliving particulate phosphorus	*C*	Biomass of cyanobacteria
B	Bacterial phosphorus	*CP*	Cyanobacteria phosphorus
F	Phytoplankton phosphorus	*CN*	Cyanobacteria nitrogen
PD_s	Sedimented particulate phosphorus	*F*	Phytoplankton biomass
DIP_s	Dissolved inorganic phosphorus in sediment	*FP*	Phytoplankton phosphorus
		FN	Phytoplankton nitrogen
		ALP	Allochtonous detrital phosphorus
		AUP	Autochtonous detrital phosphorus
		ND	Detrital nitrogen
		POSED	Organic phosphorus in sediment
		PSSED	Inorganic phosphorus in sediment
		NOSED	Organic nitrogen in sediment
		NSSED	Inorganic nitrogen in sediment

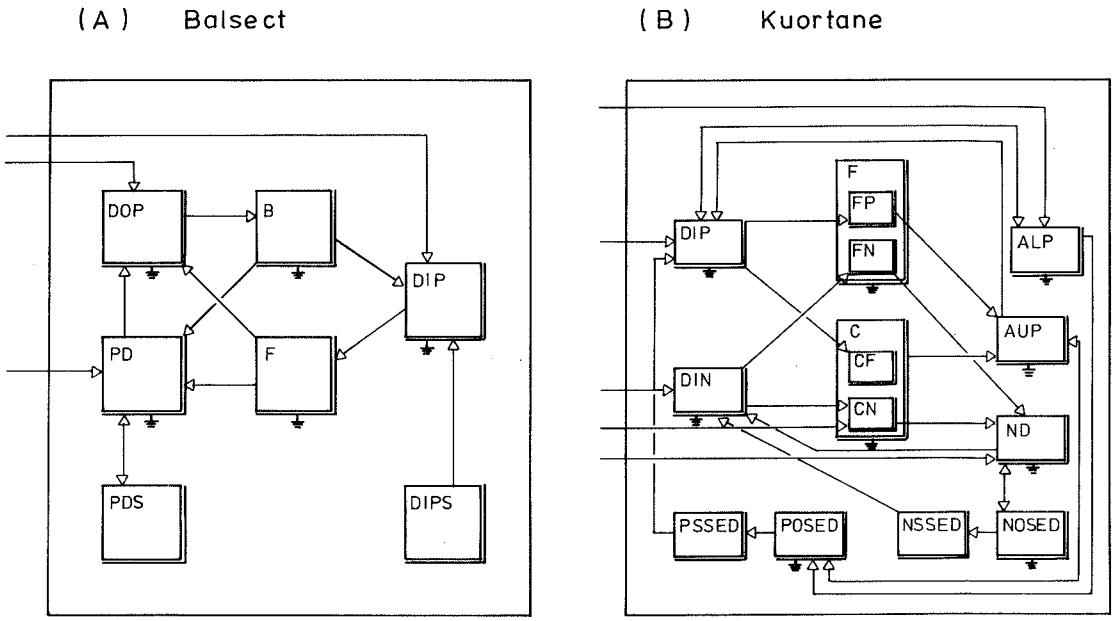

Fig. 2. Flow diagrams of the models.

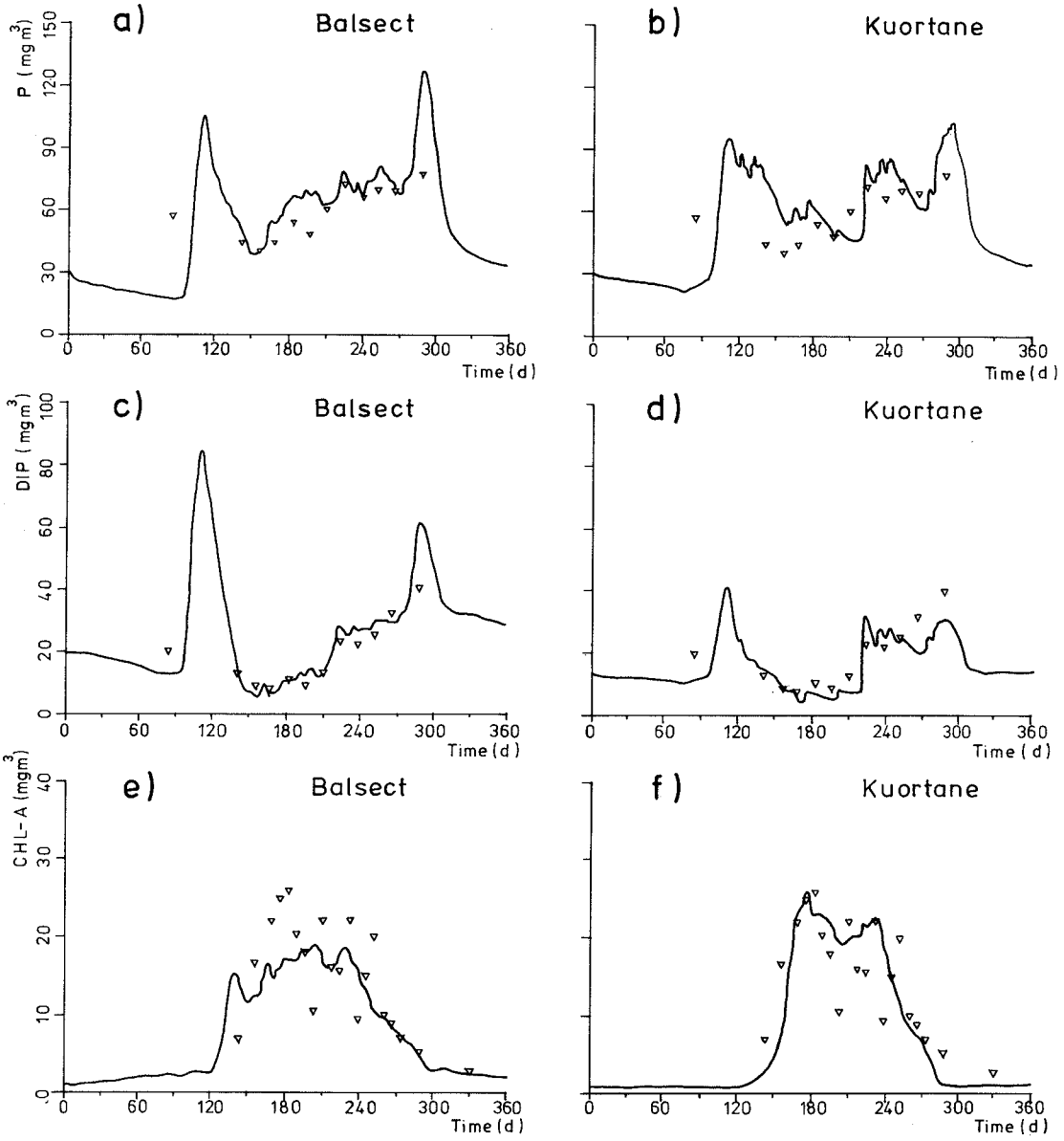

Fig. 3. Some of the calibration results of the models *BALSECT* (left) and *KUORTANE* (right) with observed data. From above: total phosphorus (a) & (b), inorganic particulate phosphorus (c) & (d) and chlorophyll-*a* (e) & (f).

5 *CASE II:* ADEQUACY OF MODELS WITH RESPECT TO INCOMPLETENESSES IN FIELD DATA

In the second case study reviewed, the adequacy of the models was assessed in terms of comparing simulated model variables observed with varying frequencies. Six variables from both models were chosen to represent following cathegories of observation type: (a) directly observed, (b) indirectly observed and (c) non-observed variables. Dissolved inorganic phosphorus (*DIP*) and total phosphorus (*TP*) represented directly observed variables. Phytoplankton phosphorus (*FP*) has been measured indirectly as cholorophyll-*a* and algal cell counts. The rates of algal phosphorus uptake (*UPT*), sedimentation (*SED*) and resuspension (*RES*) had not been measured.

The model outcomes of the six variables were compared against one another and against observations. Comparisons were made visually from plots and statistically (Varis et al. 1986b). The two most characteristic features in the results were, in very brief:

— Model simulations of the observed variables accorded far better with one another than did the unobserved ones. Also the greatest deviations in simulations of phosphorus fractions *TP* and *DIP* took place during flood periods when they were not observed.

— The original scope of modeling comprised a distinct effect on the adequacies of different model variables. The model *KUORTANE* appeared to be able to simulate algae dynamics better while *DIP* results of the *BALSECT* corresponded somewhat better the observations than did those of the *KUORTANE*. However, all processes related with eutrophication are described with similar degree of accuracy by both models.

6 CONCLUSIONS

The most general conclusions were the following:

— Both models suffer from overparametrization, i.e. they contain an excessive degree of freedom compared with the observations available. This is a very general drawback feature of the approach.

— The modeling approach can be applied for various purposes in lake ecosystem analysis as far as observed variables are concerned. The results did not suggest a good adequacy for non-observed variables. However the order of their magnitude was approximately the same. Hence, they should be considered rather as a framework.

ACKNOWLEDGEMENTS

We wish to thank the Academy of Finland and the USSR Academy of Sciences for the opportunity for co-operation. For financial support, we are acknowledged to Maa- ja vesitekniikan tuki ry.

TIIVISTELMÄ

Työssä tutkittiin Kuortaneenjärven typpi- ja fosforidynamiikkaa kahden matemaattisen simulointimallin avulla. Toinen malleista rakennettiin räätälintyönä kuvaamaan nimenomaan Kuortaneenjärven levädynamiikkaa. Toisen tavoitteena on kuvata yleisesti järvien fosforitransformaatioita. Se on alunperin muodostettu Balaton-järvelle ja sittemmin sitä on käytetty Ivankovskoe-järven analysointiin. Tulosten mukaan Kuortaneenjärven kahta allasta kuormittavat P-jakeet erosivat huomattavasti toisistaan, orgaanisten jakeiden osuus oli oleellisesti suurempi alempana sijaitsevassa pohjoisaltaassa. Nettosedimentaatio oli vain 20 % bruttosedimentaatiosta. Tässä työssä osatavoitteena oli myös tutkia ja tarkastella monimutkaisten ekologisten järvimallien tarkkuutta ja luotettavuutta. Mallien kalibrointitulokset olivat varsin tarkkoja havaittujen muuttujien osalta, mutta mallien liian suuri vapausasteiden määrä havaintoihin verrattuna näkyi selvästi niiden muuttujien kohdalla, joista ei ollut olemassa havaintoja. Myös mallintamisen tavoite heijastui mallien prosessikuvausten tarkkuuteen.

REFERENCES

Jørgensen, S.E. 1983. Ecological modeling of lakes. In: Mathematical Modeling of Water Quality: Streams, Lakes and Reservoirs (G.T. Orlob, ed.) Wiley IIASA International Series on Applied Systems Analysis. p. 337—394.

Leonov, A.V. 1985a. Studying the cycle of phosphorus forms in shallow water bodies with the aid of mathematical model (In Russian). Vodnye Resursy (Water Resources). 5:115—128.

Leonov, A.V. 1985b. Modeling and explaining the phosphorus dynamics of Lake Balaton, 1976—1979. IIASA, Research Report RR-85-3. 58 p.

Leonov, A.V., Kettunen, J. & Varis, O. 1987. Modeling phosphorus transformations in Lake Kuortaneenjärvi (in Russian). Vodnye Resursy (Water Resources). N 6:141—158.

Park, R.A., O'Neill, R.V., Bloomfield, J.A., Shugart, H.H., Booth, R.S., Koonce, J.R., Adams, M.S., Clesceri, L.S., Colon, E.M., Dettmann, E.H., Hoopes, J.A., Huff, D.D., Katz, S., Kitchell, J.F., Kohlberger, R.C., LaRoy, E.J., MacNaught, D.C., Petersen, L.J., DonScavia, J.E.T., Weiler, P.R., Wilkinson, J.W. & Zahorcak, C.S. 1974. A generalized model for simulating lake ecosystems. Simulation 23:33—50.

Stenmark, M. 1982. Nutrient cycle in Lake Kuortaneenjärvi (in Finnish, with english summary). M.Sc. thesis, Division of Water Engineering, Helsinki University of Technology. 74 p.

Varis, O. 1984. Water quality model for Lake Kuortaneenjärvi, a polyhumic Finnish lake. Aqua Fennica 14(2):179—187.

Varis, O. 1986. An analysis on the roles of limiting factors on competition facilities of blue-green algae in Lake Kuortaneenjärvi by means of simulation (in Finnish, with English abstract). M.Sc. thesis, Institute of Limnology, University of Helsinki. 72 p.

Varis, O., Kettunen, J. & Leonov, A.V. 1986a: The analysis of phosphorus bugeds in Lake Kuortaneenjärvi using a Lake Balaton model (in Finnish, with English summary). Vesitalous 27(1):16—22.

Varis, O., Kettunen, J. & Leonov, A.V. 1986b. On the adequacy of large-scale models identfied with incomplete field data — a case study with two lake models. Aqua Fennica 16(2): 157—165.

SPECIFIC FEATURES OF WATER DYNAMICS IN DIFFERENT TYPES OF LAKES

Nikolai Filatov,[1] A. Gurina, Yu. Demin, Juha Sarkkula[2] & Jorma Koponen[3]

FILATOV, N., GURINA, A., DEMIN, YU., SARKKULA, J., & KOPONEN, J. 1989. Specific features of water dynamics in different types of lakes. Publications of the Water and Environment Research Institute, National Board of Waters and the Environment, Finland, No. 3

Three-dimensional mathematical models and results of probabilistic analysis of field measurements were used to study the features of water currents in three lakes of different shape and size. Observations were used to compute vector current spectra. Typical fluctuations were distinguished in current and temperature spectra. Two different kind of numerical models were used for calculation of currents in Lake Näsijärvi (Finland). Results of these calculations were compared with measured currents.

Index words: Lake dynamics, hydrodynamic modelling

[1] Water Problem Department, Carelian Branch of the Academy of Sciences of USSR, Uritzkogo 50, SU-185003 Petrozavodsk, USSR
[2] Water and Environment Research Institute, National Board of Waters and the Environment, P.O. Box 250, SF-00101 Helsinki, Finland
[3] Reactor Laboratory, Technical Research Centre, Otakaari 3A, SF-02150 Espoo, Finland

1 INTRODUCTION

Three-dimensional mathematical models and results of probabilistic analysis of observational data have been used in this work to study specific features of synoptic and mesoscale currents in lakes of different size and shape. Lakes Ladoga and Krasnoye in the USSR and Lake Näsijärvi in Finland were chosen as the subject lakes. These lakes are located in similar physical and geographical conditions. Substantial differencies in their water dynamics may occur due to different size and shape of the lake basins. For this reason the barotropic and baroclinic Kelvin and Poincare waves, governing the formation of the dynamics of the lake water, can occur or cannot (Filatov 1983). It is of interest

to assess the possible influences of baroclinicity, bottom relief and winds, since no unique assessment has been made, so far, about the contribution of these factors to the formation of the currents in lakes.

With Lake Näsijärvi as an example, numerical experiments were carried out using two different three dimensional hydrodynamic models, originating from Sarkisjn and Demin (1986) and Simons (1983). The results of the calculations were compared with each other and an attempt was made to verify the models on the basis of current measurements made at three observation stations on Lake Näsijärvi.

Data from the observation stations served as the basis for the studies of the spectral structure of the currents and water temperature in these lakes. The subject lakes and the observation stations are indicated in Fig. 1.

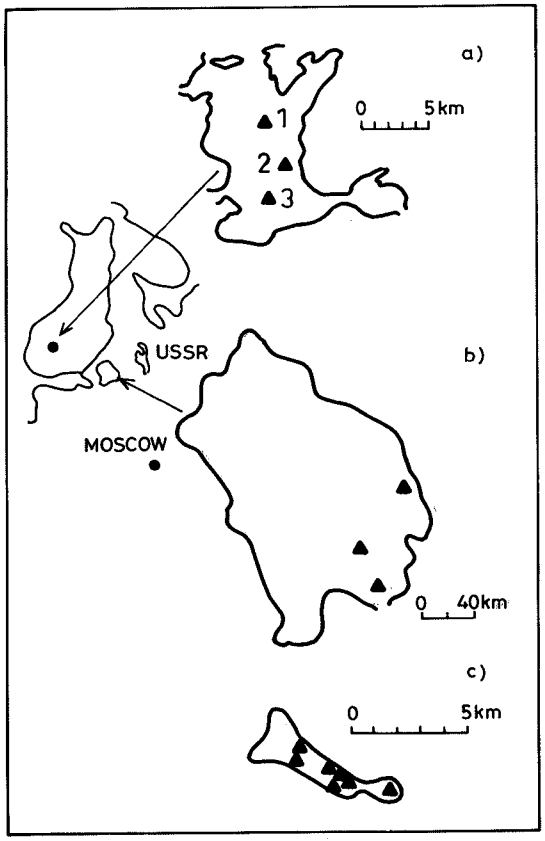

Fig. 1. Distribution of observation stations in Lake Näsijärvi (a) Lake Ladoga (b) and Lake Krasnoye (c).

2 TIME SERIES ANALYSIS OF OBSERVATION DATA

Water current and temperature observations on the lakes lasted for more than two months and the observation interval varied from 10 minutes to an hour. This made it possible to study the variability of the currents on meso- and synoptic scales. The spectra of the currents and water temperature for the subject lakes were calculated using a single technique with similar parameters (Belyshev et al. 1984). In particular, taking into account that the process of variability of the currents is vectorial, the correlative and spectral tensors of the currents were calculated with four invariant and two non-invariant characteristics.

An estimation of phase velocity for the baroclinic and barotropic modes and the Rossby deformation radius gave the results shown in Table 1.
According to Table 1 the barotropic Kelvin waves of first mode cannot exist in these lakes, since characteristic size of the lakes is smaller than the external deformation radius R. The internal Kelvin and Poincare waves can appear in large lakes such as Ladoga during summer stratification. They are possible also in Lake Näsijärvi, but in small lakes like Lake Krasnoye they are scarcely propable. Here, judging by the obtained estimates, the effect of the earth's rotation on water dynamics is small, since $L/R \ll 1$ (L is the lenght of the lake). In Lake Näsijärvi the baroclinic Kelvin and Poincare waves must be distorted substantially by an indented coastline and uneven bottom relief.

Let us consider the spectral structure of the currents and water temperature of the lakes, based on observational data (Fig. 2 and Fig. 3). The tensor of spectral density of the currents is determined by using single and reiterated Fourier transformations of correlative tensor (Belyshev et al. 1984).

The frequency-temporal spectrum (linear invariants) of the currents of Lake Näsijärvi illustrates the non-stationarity of the lake. The spectral constituents can be selected at frequencies 0.12—0.24 and near 0.45 radh^{-1}. The first can be caused by synoptic scale winds and be manifested through baroclinic Kelvin waves with a frequency higher than the local inertial frequency. On mesoscale the spectrum of the currents shows motions with a frequency close to the local inertial frequency f. These motions in the upper layer of the lake can be caused purely inertial oscillations, exited by inhomogeneous winds, and by the baroclinic Poincare waves, which exist in lakes at a distance of more than two radii of the inertia circle from the shore, i.e. at a distance more than 3 km.

It is difficult to draw the frequency temporal

Table 1. Characteristic size of the subject lakes and estimates of phase velocity Cph and the Rossby deformation radius R.

Lake	Size km^2	Average depth m	Phase velocity			
			Barotropic		Baroclinic	
			Cph ms^{-1}	R km	Cph ms^{-1}	R km
Ladoga	200 × 100	51	22	220	0.16	2—5
Näsijärvi	15 × 10	15	20	100	0.14	2—5
Krasnoye	7 × 1	10	10	100	0.04	0.5—1

spectrum for Lake Krasnoye since the currents in this lake, driven by synoptic scale winds, are episodic with a life time of a few days. Then they may cease during a period of some hours to two days.

According to the probabilistic analysis of the currents, water temperature and wind speeds for these lakes, the synoptic scale oscillations of the currents, observed at a distance of radius R in Lake Ladoga, are connected with the baroclinic Kelvin waves which show themselves here even with the absence of the synoptic scale wind fluctuations. But low-frequency oscillations exist in lakes even at a distance exceeding radius R. These motions are caused by coherent oscillations of wind speed over the lake. The characteristic increase of the velocity of the currents on the coastal zone of the lake, confined to radius R, is connected with the Kelvin waves observed in large startified lakes.

Inertial motions (Poincare waves) in lakes are of alternating character. In Lake Ladoga and Lake Näsijärvi their life-time does not exceed two-three inertial periods. They may be absent for about the same time period. As our observations show, these motions are lacking in Lake Krasnoye. The effect of the Coriolis force on the formation of the currents is determined by the wind speed oscillations. The time shift of the maxima in the low-frequency and mesoscale spectral region shows the possibility of nonlinear mechanisms for the motions at an inertial frequency.

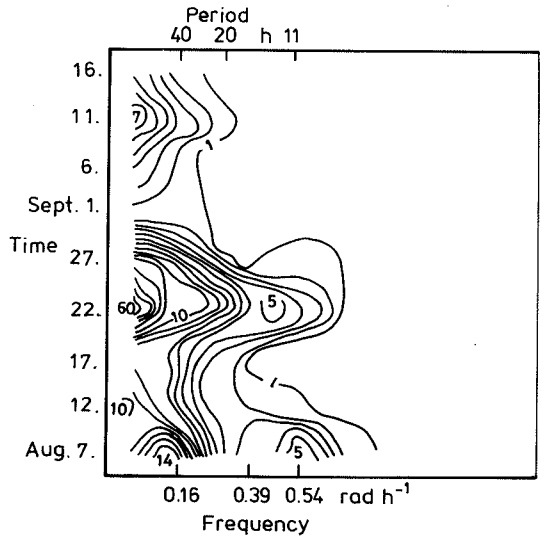

Fig. 2. Non-stationary current spectra of Lake Näsijärvi.

3 VERIFICATION AND COMPARISON OF THE HYDRODYNAMIC MODELS

So, in lakes with a horizontal size much larger than the Rossby deformation radius R, the synoptic and mesoscale currents are determined by the Kelvin and Poincare waves. Here the nonlinear effects in the formations of specific currents in the coastal zone, confined to R, are substantial. In mathematical modelling of lake dynamics it is essential to thoroughly resolve the coastal zone by correct choice of the grid size and to emphasize the parametrization of sub-grid processes and, in particular, the choice of coefficients for horizontal and vertical turbulent exchange Kh and Kz. An overestimation of Kh leads to smoothing the calculated temperature fields and loosing the water circulation (cyclonic circulation). The Kz coefficient was chosen from preliminary calculations based on observations of the vertical distribution of currents and temperature.

In the moderate-sized lake Näsijärvi the spectrum of motions is typical of that for large lakes, and the field observations are available for calibrating and verificating the two models mentioned

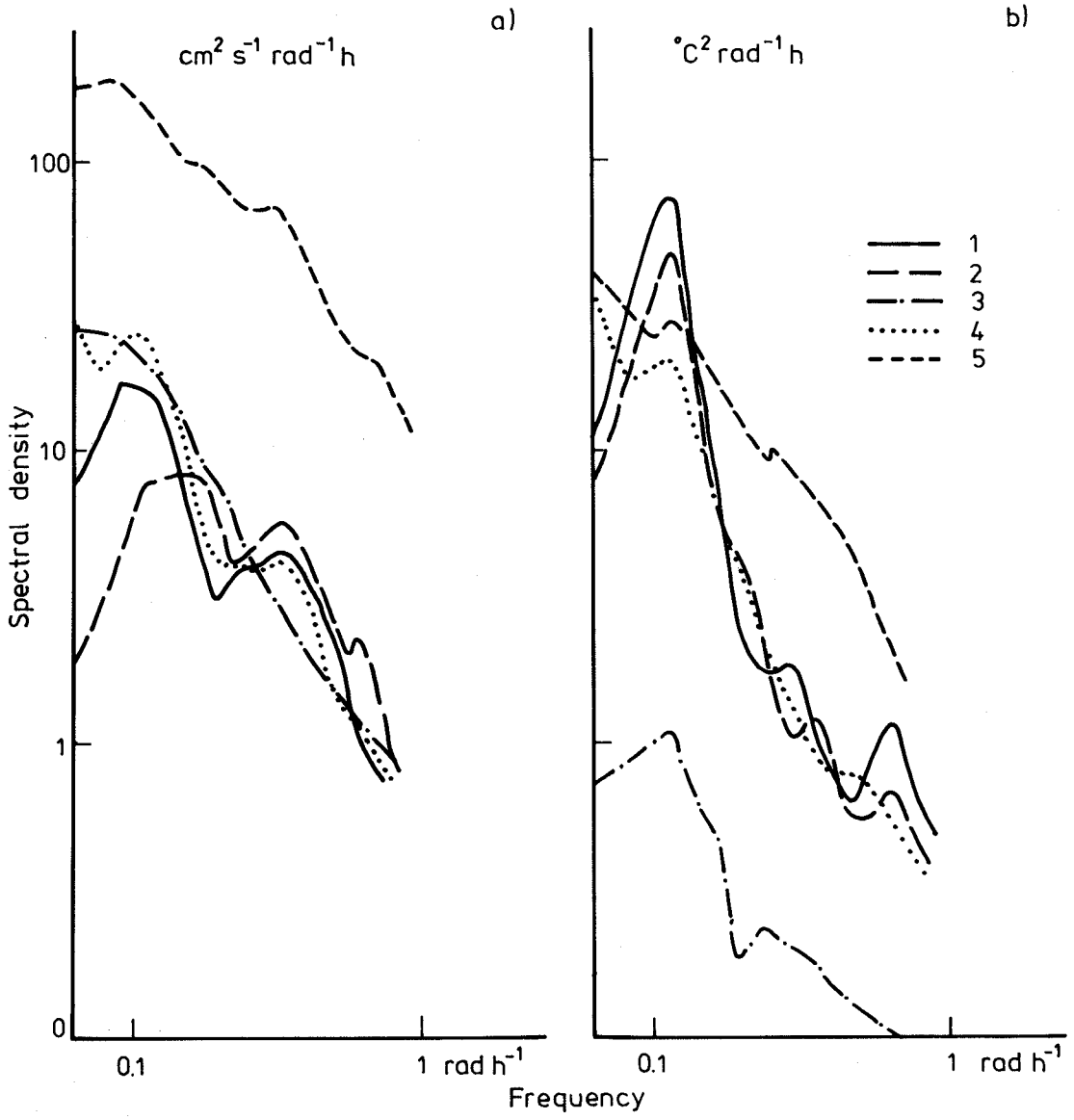

Fig. 3. Spectra of currents (a) and water temperature (b) of Lake Näsijärvi (1, 2 and 3 according to observation stations), Lake Krasnoye (4) and Lake Ladoga (5).

earlier. The water level and the currents of Lake Näsijärvi were calculated using a nonlinear multilayer model (Sarkisjn and Demin 1986), which has been earlier used to calculate the currents of Lakes Ladoga, Sevan and Biva. The coefficients for horizontal turbulent exchange were first estimated with Hasselberg and Kolmogorov's formulae, using the spectra of the fluctuation of the currents (Filatov 1983). The Kh values ranged between 103 and 105 cms^{-1}, differing for the coastal and open-water zones of the lake by an order of magnitude. However, this fact was neglected in the preliminary calculations. The most acceptable estimate for Kz was 1—10 cms^{-1}, based on observational data and preliminary calculations of the thickness of the upper Ekman layer.

Results of calculations with the other model (Simons 1980) are published by Koponen et al.

(1986). Calculations were performed with a grid size of 1000 meters, and the lake was vertically devided into six layers. The grid step was much smaller than the internal radius of the Rossby deformation, which made it possible to reveal the effects caused by the internal Kelvin waves. The time step was 55 seconds, which enabled one to determine the effects caused by the Poincare waves, in time scales equal to or less than the period of inertia for the lake width (equal to 13,5 hours). However, the spatial resolution of the grid did not permit one to describe these motions.

For the upper layer the coefficient of horizontal turbulent pulse exchange was taken 8 cm^2s^{-1} and for the thermocline area 1 cm^2s^{-1}. The coefficients of horizontal momentum exchange was taken 104 cm^2s^{-1}. The field of currents was calculated, by the two models, for a period of thermal stratification (August) with a wind of 4 ms^{-1} in the direction of 190°. In the case of the diagnostic model the currents were calculated from the field of water temperature, obtained from Simons' model, with a gried size of 500 meters at eight depths between 0 and 25 meters. The coefficient of vertical turbulent exchange was assumed to be constant and equal to 10 cm^2s^{-1}.

The results from the diagnostic model and from Simons' model are compared with the observations made simultaneously at three stations at 2,5 and 8 meters depth.

Figure 4 shows the results of the calculated lake water level. Deviations from the level of undisturbed state vary between +30 and −20 mm (Simons' model) and between +13 and −10 mm (diagnostic model), i.e. the velocity from the diagnostic model must be somewhat less. The topography of the free surface does not differ qualitatively between the models.

Table 2 gives the results of the statistical analysis of the calculated velocity fields. The velocity was averaged over a field of 75 points at 2,5 meters depth and of 61 points at 8 meters depth.

The results show that the average and maximum current velocities from Simons' model are higher than the ones from the diagnostic model at both depths. An analysis of the fields of the currents (Fig. 5.), calculated with the models, shows that in the upper 0—5 meter layer the wind-driven currents prevail, and beneath this layer the effects of baroclinicity and bottom relief contribute most.

The modelled currents were compared with observations made at the three stations. Data, obser-

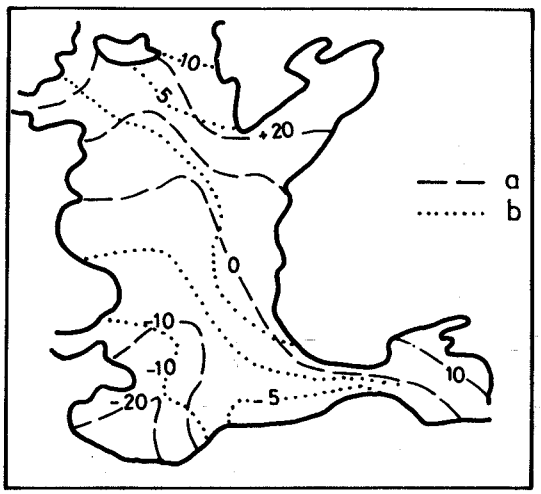

Fig. 4. Level of free surface (mm) of Lake Näsijärvi computed with Simons' model (a) and the diagnostic model (b).

Table 2. Modelled average values of current velocity (u,v), mean velocity (v) and maximum velocity vmax in Lake Näsijärvi at 2,5 and 8 meters depth with wind direction 190° and speed 4 ms^{-1}.

Depth m	Parameter cms^{-1}	Model	
		Simons	Diagnostic
2,5	u	2,5	0,2
	v	3,4	0,7
	v	4,7	3,3
	vmax	16	9
8	u	-0.5	-0.9
	v	2,8	0.2
	v	2.5	1,7
	vmax	8	7

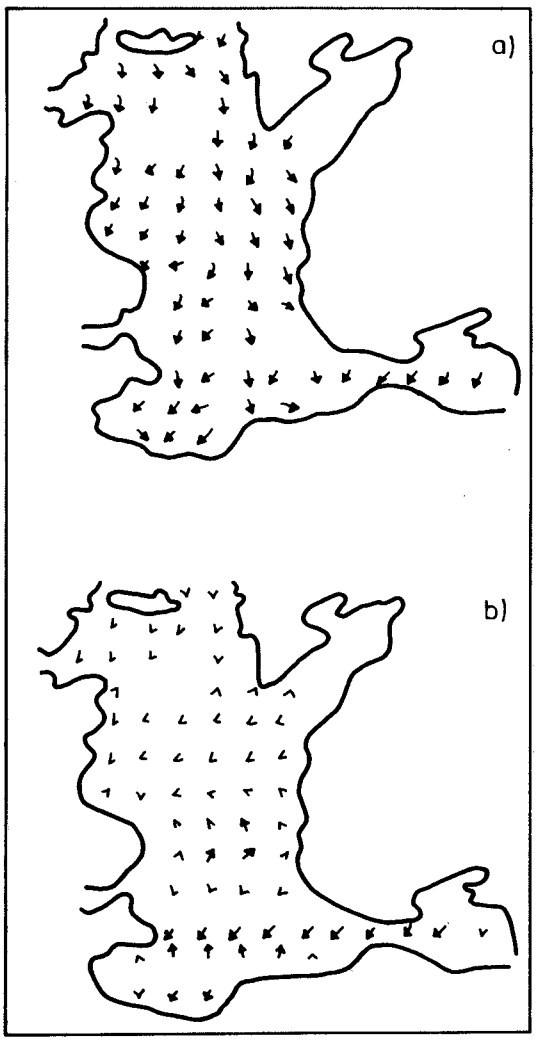

Fig. 5. Currents of Lake Näsijärvi at 8 meters depth computed with Simons' model (a) and the diagnostic model (b).

ved every 10 minutes, was averaged over 30 hours, which corresponds to the time period needed for the currents to form (according to Simons' model). Table 3 lists the results of this comparison. Since the location of the observation stations did not coincide with the grid poinst, the direction and velocity of the currents were averaged over the values at 3—4 grid points.

As seen from Table 3, the observed current velocity is higher in the surface layer than the modelled one. The results of the measurements in the upper layer show that the water flow mainly at an angle of 20—40° with respect to wind direction, the variability of the currents is small and no inertial and other oscillations were observed here in this period. For 8 meters depth the observed and modelled current velocities and directions coincide.

4 CONCLUSION

Studies have been carried out about the currents in lakes of different size and shape. The transformation of the spectra of currents, depending on the hydrometeorological conditions as well as on the shape and size of the lake, has been shown.

The currents in Lake Näsijärvi were calculated for a stratification period using nonlinear diagnostic and prognostic models. Comparisons have shown that, qualitatively, the results of calculations of velocity fields are not controversial and agree reasonably well with the 30 hour averaged data from the observation stations. For a more correct verification of the models, more observation stations are needed, which will take into account specific circulations of the lake water. The

Table 3. Simulated and observed currents in Lake Näsijärvi over a 30 hour period at different observation stations.

Depth m	Station	Simons model		Diagnostic model		Field data	
		dir. °	velocity $cm\,s^{-1}$	dir. °	velocity $cm\,s^{-1}$	dir. °	velocity $cm\,s^{-1}$
2.5	1	30	8	100	5	50	16
	2	40	8	300	3	300	8
	3	50	9	190	8	40	16
8	1	190	5	190	3	140	5
	2	270	5	280	3	190	3
	3	280	4	190	4	330	4

calculations with the models showed that the amount of observation stations should not be less than 7.

Calculation have also shown that in the upper 0—5 meter layer the wind effects prevail, and beneath it the combined effects of baroclinicity and bottom relief are observed.

ACKNOWLEDGEMENTS

The work was done in the framework of the cooperation between the Academy of Sciences of the USSR and the Finnish Academy.

N. Filatov, A. Gurina and Yu. Demin were responsible for the spectral analysis of the observed data as well as for the runs with the diagnostic model. J. Koponen made the computation with Simons' model and J. Sarkkula was responsible for the current measurements and data processing in Lake Näsijärvi.

REFERENCES

Belyshev, A., Klevanzov, J. & Rojkov, V. 1984. A statistical analysis of ocean currents. Gidrometeoizdat. 264 p.

Filatov, N. 1983. Dynamics of lakes. Gidrometeoizdat. 166 p. Sarkisjan, A. & Demin, J. 1986. Methods and results of simulations of currents in ocean. Gidrometeoizdat. 151 p.

Simons, T. 1980. Circulation models of lakes and inland seas. Canadian bulletin of Fisheries ans Aquatic Sciences 203. 145 p.

Virtanen, M., Koponen, J., Dahlbo, K. & Sarkkula, J. 1986. Three dimensional water quality-transport model compared with field observations. Ecological modelling, 31:185—199.